NAVAL POSTGRADUATE SCHOOL
Monterey, California

THESIS

J5496

Flow Visualization of the Airwake Around
a Model of a DD-963 Class Destroyer
in a Simulated Atmospheric Boundary Layer

by

Michael K. Johns

September 1988

Thesis Advisor: J. Val Healey

Approved for public release; distribution is unlimited.

REPORT DOCUMENTATION PAGE

1a Report Security Classification Unclassified		1b Restrictive Markings
2a Security Classification Authority		3 Distribution Availability of Report
2b Declassification/Downgrading Schedule		Approved for public release; distribution is unlimited.
4 Performing Organization Report Number(s)		5 Monitoring Organization Report Number(s)

6a Name of Performing Organization Naval Postgraduate School	6b Office Symbol (If Applicable) 67	7a Name of Monitoring Organization Naval Postgraduate School
6c Address (city, state, and ZIP code) Monterey, CA 93943-5000		7b Address (city, state, and ZIP code) Monterey, CA 93943-5000
8a Name of Funding/Sponsoring Organization	8b Office Symbol (If Applicable)	9 Procurement Instrument Identification Number
8c Address (city, state, and ZIP code)		10 Source of Funding Numbers

Program Element Number	Project No	Task No	Work Unit Accession No

11 Title (Include Security Classification) FLOW VISUALIZATION OF THE AIRWAKE AROUND A MODEL OF A DD-963 CLASS DESTROYER IN A SIMULATED ATMOSPHERIC BOUNDARY LAYER

12 Personal Author(s) Johns, Michael K.

13a Type of Report Master's Thesis	13b Time Covered From To	14 Date of Report (year, month,day) 1988, September	15 Page Count 58

16 Supplementary Notation The views expressed in this thesis are those of the author and do not reflect the official policy or position of the Department of Defense or the U.S. Government.

17 Cosati Codes			18 Subject Terms (continue on reverse if necessary and identify by block number)
Field	Group	Subgroup	Flow Visualization, Simulated Atmospheric Boundary Layer, Helium Bubble Flow Visualization, Smoke Flow Visualization, Spruance Class Destroyer

19 Abstract (continue on reverse if necessary and identify by block number)
This study is part of a longer-term project to map the airwakes of model ships for scaling to full size and use in helicopter simulators to provide an alternative to at-sea dynamic interface testing utilizing the Naval Postgraduate School flow visualization tunnel modified to simulate the open ocean atmospheric boundary layer. A detailed analysis has been made of the airflow near the flight deck of the DD-963 in a stationary mode, using helium bubble, smoke, photographic and video equipment. The results show that the primary variable in the airwake is the yaw angle of the ship; pitch and roll having a lesser influence. Some highly complex flow patterns have been observed above the flight deck. For example, at zero degrees yaw, the airflow along the center line of the ship flows over the hangar and splits: the higher level of the flow continues aft and the lower level proceeds downwards towards the deck and turns back towards the hangar; this flow further splits, heading towards port and starboard, curls upward almost to the hangar "roof" level and finally flows downwind in two streams along paths close to both sides of the ship. This pattern becomes displaced to one side of the ship or other, depending on the yaw angle.

20 Distribution/Availability of Abstract [X] unclassified/unlimited ☐ same as report ☐ DTIC users	21 Abstract Security Classification Unclassified	
22a Name of Responsible Individual Prof. J. Val Healey	22b Telephone (Include Area code) (408) 646-2804	22c Office Symbol 67He

Flow Visualization of the Airwake
Around a Model of a DD-963 Class
Destroyer in a Simulated Atmospheric
Boundary Layer

by

Michael K. Johns
Lieutenant Commander, United States Navy
B.A., Wichita State University, 1975

Submitted in partial fulfillment of the
requirements for the degree of

MASTER OF SCIENCE IN AERONAUTICAL ENGINEERING

from the

NAVAL POSTGRADUATE SCHOOL
September 1988

ABSTRACT

This study is part of a longer-term project to map the airwakes of model ships for scaling to full size and use in helicopter simulators to provide an alternative to at-sea dynamic interface testing utilizing the Naval Postgraduate School flow visualization tunnel modified to simulate the open ocean atmospheric boundary layer. A detailed flow visualization analysis has been made of the airflow near the flight deck of the DD-963 in a stationary mode, using helium bubble, smoke, photographic and video equipment. The results show that the primary variable in the airwake is the yaw angle of the ship; pitch and roll having a lesser influence. Some highly complex flow patterns have been observed above the flight deck. For example, at zero degrees yaw, the airflow along the center line of the ship flows over the hangar and splits: the higher level of the flow continues aft and the lower level proceeds downwards towards the deck and turns back towards the hangar; this flow further splits, heading towards port and starboard, curls upward almost to the hangar "roof" level and finally flows downwind in two streams along paths close to both sides of the ship. This pattern becomes displaced to one side of the ship or other, depending on the yaw angle.

C.1

TABLE OF CONTENTS

LIST OF TABLES

LIST OF FIGURES

ACKNOWLEDGEMENTS

I. INTRODUCTION

In the past twenty years there has been a dramatic growth in the use of helicopters in conjunction with non-aviation ships in naval operations. Many new and major problems arise from such operations, particularly during the landing phase in the presence of high winds and stormy seas. Excessive motions of the ship combined with a highly turbulent airwake from the ship's superstructure can make landing a hazardous process. Furthermore, the very large number of helicopters and ships, each with its own more or less unique shape, size and handling characteristics, leads to several hundred helicopter/ship combinations. At present, the safe operating envelopes are determined by the Naval Air Test Center (NATC) at sea, a slow, laborious and expensive process. Even if the very high cost of about $150,000 per combination is ignored, it is estimated that, due to unavailability of the ships, all the operating envelopes cannot be determined this century. These problems led to the suggestion that simulation of the interface might permit determination of the safest wind envelopes.

In a recent study, Healey [Ref. 1] has attempted to determine the feasibility of the simulation by examining the current state of predicting

- the wind state in a neutral atmosphere, representing the freestream flow to the ship in high wind conditions.
- the ship motion in the sea that is likely to accompany this atmosphere.
- the ship airwake arising from both the wind and the ship motion.
- the helicopter response in this highly turbulent flowfield,

and finally, if all the above are predictable,

- can current computers handle the simulation?

1

It was concluded that while further work was necessary on both the existing ship motion prediction program and the turbulence modeling of helicopters, the ship airwake is virtually unknown and attempts at its analysis to date have been faulty. Knowledge of ship airwakes is desirable for other good reasons: from NATC tests, it is known that ship anemometers give readings that are inaccurate because of interference of the airwake with the freestream airflow. Furthermore, immediately after launch, missiles lack the speed for good control and are, to a degree, at the mercy of the ship airwake. Knowledge of the wake can lead to a resolution of such problems.

In the high-speed neutrally stable wind regime of interest in the present problem, the earth's atmosphere is a sheared turbulent boundary layer, and there is abundant evidence that it can be simulated in a special wind tunnel, such as the environmental one at Colorado State University. In the 1960's an interest was developed in generating suitable boundary layers in ordinary wind tunnels and a method was developed by Counihan in England. Detailed descriptions of such tunnels are given by J. E. Cermak [Ref. 2]. The Counihan and other methods are described by Davenport [Ref. 3].

Furthermore, the combined airwake due to the motion of the ship and the freestream airflow can be modeled in this tunnel with equality of Strouhal number, while maintaining the minimum Reynolds number of about 10,000 that is necessary for viscous/inertia similarity. The current study does not include simulation of the ship motion and, hence equality of Strouhal numbers is not required. Provided the ship superstructure has no significant round-forebody components, this Reynolds number should be adequate.

Unfortunately, most past efforts, for example White and Chaddock [Ref. 4] (see also paper by Loezos [Ref. 5]), Garnett [Refs. 6, 7, and 8], Hurst and Newman [Ref. 9], etc. have used ordinary wind tunnels with essentially uniform flows and turbulence intensities of one half percent or thereabouts. Apart from the Naval Postgraduate School, the only other institutions known to the author, and his faculty advisor, using sheared turbulent layers in conjunction with ship airwakes are the National Aerospace Laboratory (NLR) in the Netherlands and the National Maritime Institute in England.

The program underway at the Naval Postgraduate School (NPS) has the longer-term aim of making detailed air-wake maps of model ships and scaling the results to the full-size. With this in mind, various ship models up to 4' (1.2 m) long have been acquired for flow-visualization purposes. It is hoped to expand the current width of the flow-visualization tunnel of 5' (1.5 m) to 8' (2.4 m) to increase the resolution of the measurements. Meantime, detailed flow visualization studies on various models are being conducted.

The ship airwake is expected to be a function of the following:

- The wind condition: its mean speed profile, turbulence intensity, longitudinal length scale of the turbulence, and spectrum function.
- The wind/ship speed ratio, because it affects the turbulence intensity.
- The relative wind direction and
- The ship motion.

According to the E.S.D.U. [Ref. 10], specification of the mean wind speed u, the elevation above the mean obstruction height z and the surface roughness is sufficient to determine the turbulence intensity, longitudinal length scale and the spectrum function for the neutral atmosphere. Over rough seas [Ref. 3], the surface roughness is typically in the range 0.001 to 0.01 meters and the distance of the deck

or flight deck of a ship above the mean wave height provides the elevation. Thus, sufficient information exists to determine, in a statistical sense, the likely turbulence intensity, length scales and spectrum function for the sea state accompanying that wind.

According to Plate [Ref. 11], modeling the velocity profile in the form $u/U = (z/Z)^n$, (where U is the velocity at the top of the boundary layer at elevation Z) and the turbulence intensity in a wind tunnel appears to be sufficient to ensure correct modeling of the environment. Davenport [Ref. 3] gives typical values of the index n for rough sea 0.11 to 0.15, corresponding to surface roughnesses in the range 0.001 m to 0.01 m.

More thorough background discussions of the atmospheric boundary layer and its simulation relating to the ship airwake may be found in Healey, Bolinger, Biskaduros, and Daley [Refs. 1, 12, 13, and 14].

II. SHIPBOARD OPERATIONS

The DD-963 "Spruance" class destroyer is currently the U.S. Navy's surface fleet standard for anti-submarine warfare (ASW). Built from the keel up with ASW in mind, 31 have been constructed since USS Spruance was first laid down in 1972. The 7800 ton displacement ship is 563' (171m) long, and has a beam of 55' (16.75m). (See Figure 1).

An integral part of the ship's ASW weapon system, along with many other missions, is its aviation capability. Specifically, the operational deployment of the Light Airborne Multi-Purpose System (LAMPS), consisting of the SH-2F helicopter and associated shipboard and aircraft electronics. In addition, a program is ongoing to incrementally add the LAMPS MKIII system to the Spruance fleet. Utilizing the SH-60B helicopter, the MKIII system employs the Recovery, Assist, Secure and Traverse System (RAST) to assist in the landing and on deck movements of the aircraft. Other United States Naval helicopters that are certified to land on the Spruance include the SH-3, and the CH-46.
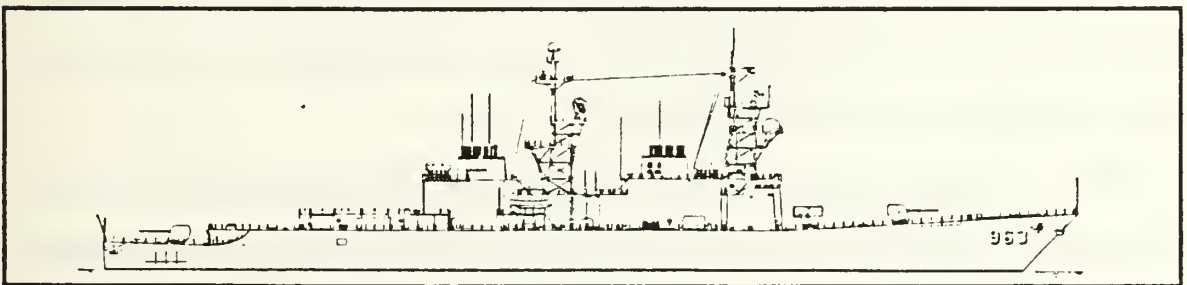
Figure 1. USS Spruance, DD-963, Profile View. [Ref. 15]

The flight deck is located on the 'O2 level' aft, 33' (10 m) above the waterline with the landing area approximately 52 X 42' (15.6 x 12.6 m), and positioned 17.5'

(5.3 m) aft of the hangar. The hangar is 49' long, 26' wide and 18' high (14.9 x 7.9 x 5.5 m) with the exhaust stacks for the aft two gas turbine engines situated on top, starboard side. (See Figure 2).
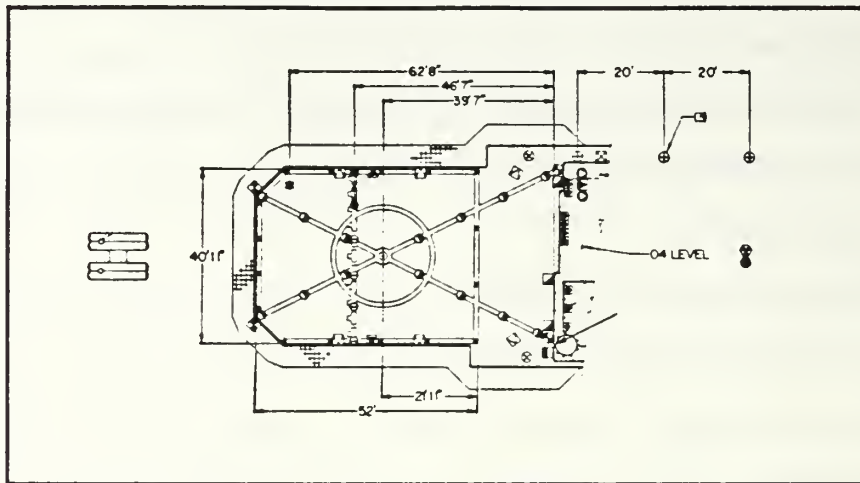
Figure 2.   Main Flight Deck, DD-963 class, Plan View. [Ref. 16]

Aviation operations on the Spruance are not restricted to the primary flight deck. There are two 10 X 20' (3 x 6 m) vertical replenishment (VERTREP) areas that are located on the O1 level forward and the main deck aft. See Figures 3 and 4. They are certified for operations involving the transfers of underslung loads from hovering helicopter. Because of time constraints, however, this study focused primarily on the main flight deck. Further study would be required to define the airflows specific to the VERTREP decks.

Prior to landing a helicopter the ship's deck officer must first position the ship to obtain relative winds that are at least within published limitations and preferably optimum for pilots' preferences and overall weather conditions. Figures 5 - 7 are three representative wind envelopes for the SH-2F. Each applies to a different set of weather and aircraft conditions; Figure 5 applies to day, starboard approaches,
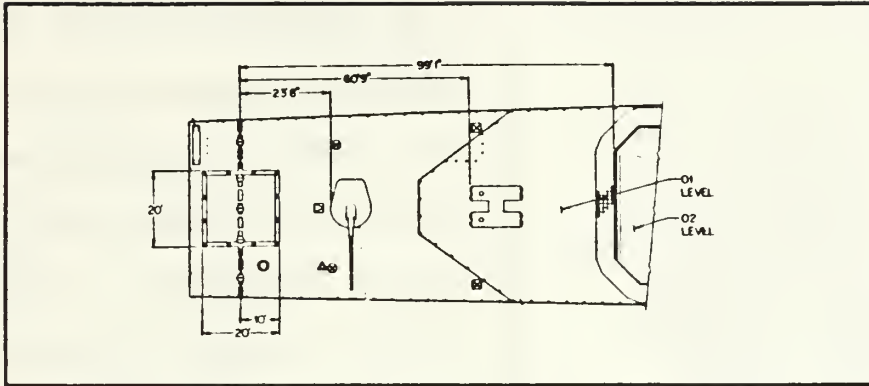
Figure 3.   Aft VERTREP Area, DD-963 Class. [Ref. 16]
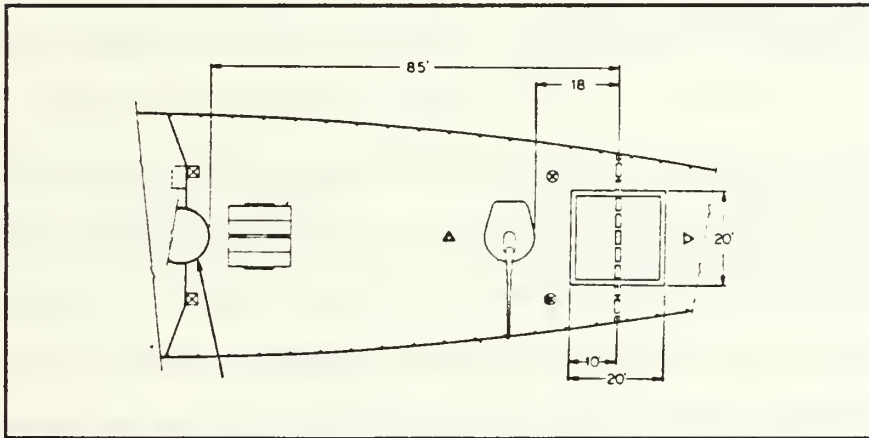
Figure 4.   Forward VERTREP Area, DD-963 Class. [Ref. 16]

7
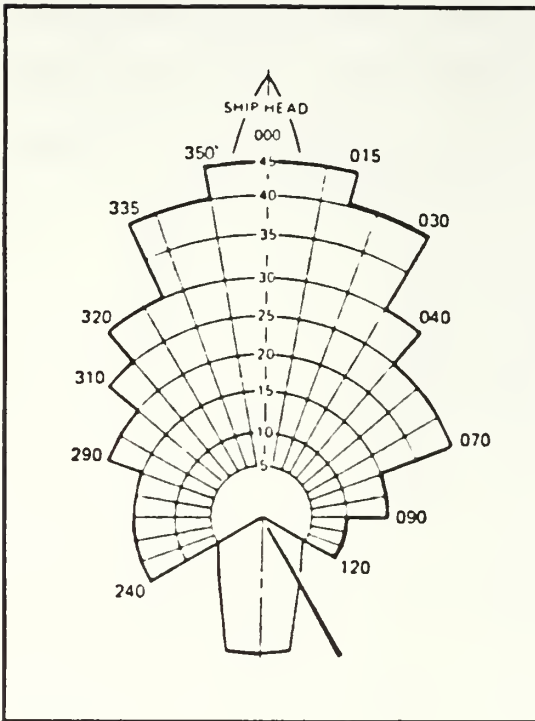
Figure 5. Typical DD-963
Operating Envelope - Day,
Starboard Approach [Ref. 17]

i.e., approaches from the starboard side; Figure 6 to night, port approaches, and Figure 7 to day, starboard approaches with inoperative aircraft automatic stabilization equipment (ASE) or hydraulic boost. Note how the envelopes become more restrictive during night or with an aircraft malfunction. In addition to relative winds, the ship must be within established pitch and roll limits. The standard day and night approaches require roll to be from zero to five degrees and pitch from zero to four degrees, and with ASE off, zero to five degrees for roll and zero to two degrees for pitch. Pitch limitations are considered to be the most critical because of the fore and aft movement of the hangar face while the aircraft is in a hover over the flight deck; such motions can be quite disorienting to the pilot. In average conditions, however, pitch magnitudes in excess of two degrees are infrequently encountered.

Ship roll is more easily tolerated within limits because the pilot can maintain a somewhat fixed position over the flight deck relative to the hangar and simply coordinate his landings/takeoffs to coincide with a level ship position. As would be expected, combining high roll and pitch magnitudes with night operations or other adverse conditions such as an aircraft malfunction make the landing sequence a very critical operation. Pilots strive to make the transition between forward flight aft of

the ship and landing as quick as possible and would desire optimum winds with the least amount of turbulence.
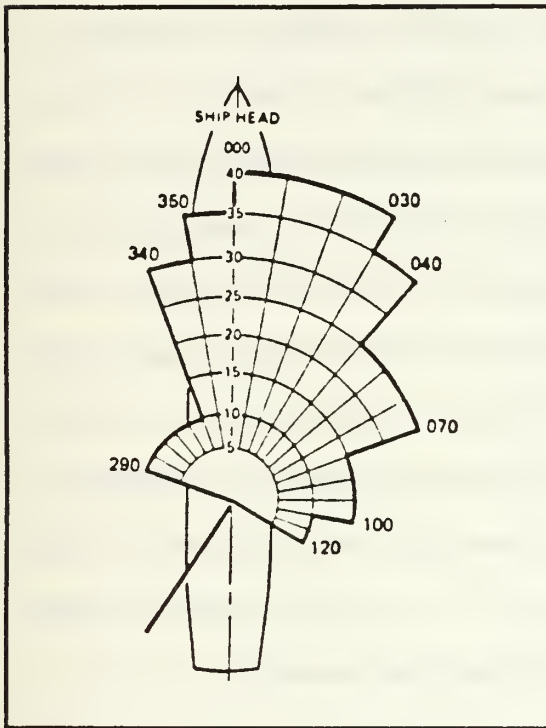
Figure 6. Typical DD-963
Operating Envelope - Night,
Port Approach [Ref.17]
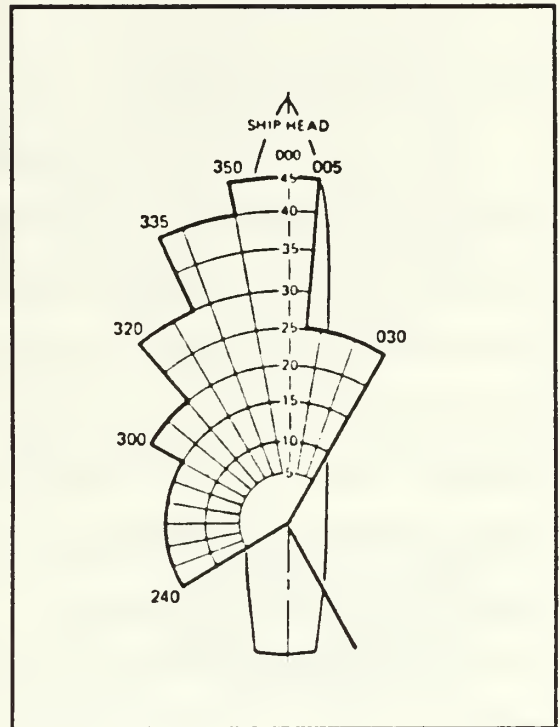
Figure 7. Typical DD-963
Operating Envelope - Day
Starboard Approach with ASE
or Boost off. [Ref. 17]

Despite the wide range in the limitations, helicopter pilots generally prefer to fly standard day approaches from the starboard side with the relative winds coming from approximately 330° (000° being straight ahead) at a moderate velocity of about 15-25 knots, which is well within the wind envelope (Figure 5). This landing configuration provides the best visibility for the aircraft commander who normally
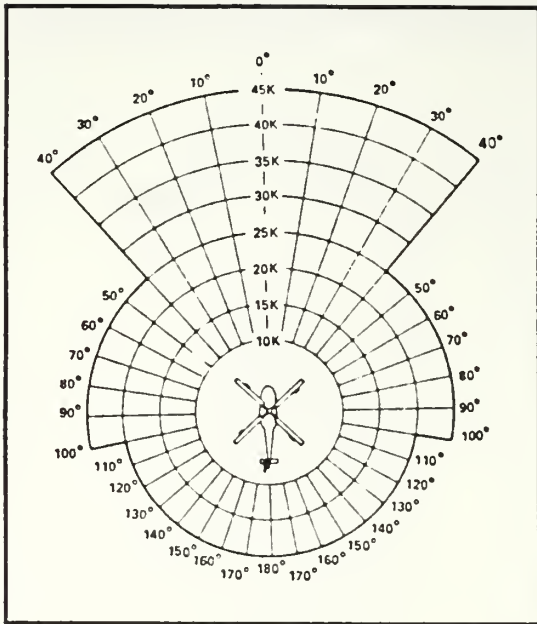
Figure 8.   Typical SH-2F Operating Envelope - Maximum Wind for Starting or Stopping Rotors. [Ref. 17]

sits in the right-hand seat, and provides optimum winds if something happened which would require a waveoff or single engine flight transition. In addition to approach wind envelopes, there are also prescribed wind limitations for rotor engagement and disengagement. (Figure 8). When the helicopters rotor system is at a relatively slow speed during starting and stopping, it is extremely susceptible to high magnitude flapping movements due to turbulent air. The envelope is modified when gusty conditions are encountered:

Limiting velocities indicated on wind charts represent maximum for steady state, nonturbulent winds. During gusty wind conditions and/or for pitching deck, if the gust speed is 10 knots or more, reduce the maximum winds allowed for rotor engagement/disengagement by 10 knots in all quadrants. [Ref. 17]

Pilot preferences for starting and stopping rotors are almost universally to have light to moderate winds on the nose of the helicopter.

III. EXPERIMENTAL APPARATUS

A. WIND TUNNEL

This study utilized the NPS flow visualization wind tunnel modified to simulate the atmospheric boundary layer for airwake studies.

The tunnel is open circuit, originally designed for smoke flow visualization. Air enters a 15 X 15' (4.5 x 4.5 m) inlet and passes through a three inch (7.5 cm) honeycomb and mesh screen. A 9:1 ratio square bell contraction cone directs the flow into a 5 X 5' (1.5 x 1.5 m), 22' (6.7 m) long test section. (See Figure 9). After the test section the flow transitions to a circular fan section where a variable pitch fan is used to force the flow and control its speed. The flow is then exhausted to the atmosphere.

An observation room is located on one side of the test section housing the necessary flow visualization equipment. A 5.2 X 3.5' (1.6 x 1.1 m) window provides the primary viewing area from the observation room, along with a 5X2' (1.5 x 0.6 m) window on the opposite wall and a 16X18" (40 x 45.7 cm) window directly above the model. The main viewing window provides ample area to photograph the model from many angles, and from as low as four inches from the test section floor. Cut into the floor is a 4.25' (1.3 m) diameter circular platform with a removable section cutout to fit the ship hull. All opaque surfaces are painted flat black to maintain low light reflectivity.

As discussed earlier, the tunnel was modified to simulate the atmospheric boundary layer. A boundary layer of 30" (0.76 m) thickness was considered
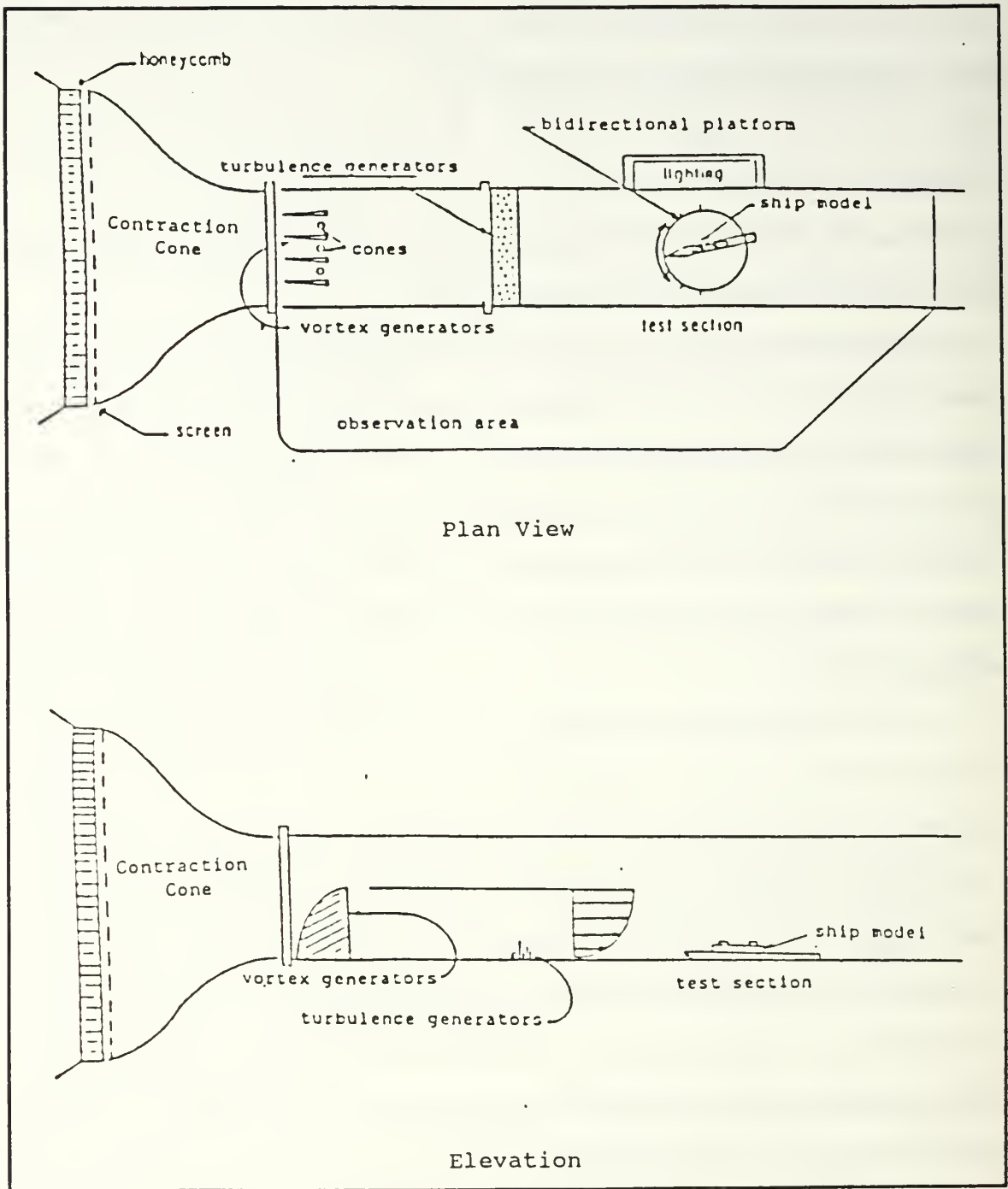
Figure 9. NPS Flow Visualization Tunnel. [Ref. 12]

12

sufficient, since the height above the tunnel floor of any model was unlikely to exceed 20-25% of that. There are numerous methods of setting up sheared turbulent boundary layers and the Counihan one was chosen because of its inherent simplicity. The four vortex generators that generate the shear and part of the turbulence are of the quarter-elliptical shape when viewed from the side, are 2.5' (0.75 m) high, one half of that in the flow direction and 3" (75 mm) maximum thickness at the leeward side of the base, and are made of aluminum and styrofoam. (Figure 9). Viewed from above or the windward side, the generators are wedge-shaped. In addition, three 30" (0.76 m) high, two inch (5.1 cm) diameter tapered cones were added to refine the horizontal velocity profile. The remaining part of the turbulence was generated by randomly placing various lengths (1-6 inches (2.54 - 15.2 cm)) of 3/8" (9.5 mm) dowels vertically over a 18" X 5' (45.7 x 1.5 m) section of the tunnel floor just forward of the model. Measurements of the turbulence intensity across the section now showed typically 12 to 13%, at the 2" (50 mm) levels, and this was considered adequate. Bolinger [Ref. 12] details the tunnel modifications and Tables 1, and 2, reprinted from Bolinger, provide test section velocity and turbulence intensity data.

With this boundary layer, some earlier studies were conducted on simple blocks, combinations of blocks and simple ship-like structures initially and, more recently, on models of the USS Lexington and Tarawa.

TABLE 1. TEST SECTION VELOCITY DATA. [Ref. 12]

x*	Z- Height above floor (inches)
	2.00	3.00	4.00	8.00	12.00	16.00	19.00	25.00	30.00
6.00	6.21	6.36	6.63	7.81	7.84	8.13	8.44	8.61	9.15
9.00	6.32	6.35	6.84	7.89	7.78	8.00	8.40	8.60	9.23
12.00	6.24	6.40	6.88	7.83	7.80	8.09	8.37	8.65	9.16
15.00	6.29	6.39	6.78	7.65	7.88	8.25	8.40	8.65	9.21
18.00	6.23	6.41	6.58	7.53	7.90	8.17	8.41	8.43	9.07
21.00	6.34	6.43	6.70	7.80	8.05	8.16	8.53	8.59	9.27
24.00	6.30	6.13	6.74	7.79	8.01	8.09	8.49	8.51	9.24
27.00	6.28	6.26	6.85	7.77	7.96	8.05	8.41	8.60	9.01
30.00	6.24	6.22	6.77	7.85	7.89	8.01	8.28	8.58	9.21
33.00	6.22	6.30	6.65	7.79	7.84	7.98	8.38	8.56	8.96
36.00	6.31	6.10	6.71	7.56	7.78	8.06	8.43	8.64	8.91
39.00	6.29	6.17	6.74	7.66	7.80	8.09	8.44	8.59	9.21
42.00	6.26	6.20	6.72	7.76	7.82	8.07	8.34	8.57	8.98
45.00	6.33	6.37	6.83	7.76	7.85	8.06	8.34	8.63	9.03
48.00	6.25	6.34	6.73	7.84	7.95	8.27	8.38	8.64	8.83
51.00	6.25	6.27	6.79	7.77	8.01	8.24	8.44	8.77	9.08
AVE.	6.27	6.29	6.75	7.75	7.89	8.11	8.41	8.60	9.10
V/Vo	0.68	0.69	0.74	0.85	0.87	0.89	0.92	0.95	1.00
SIGMA	0.04	0.09	0.08	0.09	0.08	0.08	0.06	0.07	0.13

Vo at 30 inches = 9.1 ft/sec
* transverse position from far wall in inches

14

TABLE 2. TEST SECTION TURBULENCE INTENSITY DATA (%).
[Ref. 12]

X*	Z- Height above floor (inches)								
	2.00	3.00	4.00	8.00	12.00	16.00	19.00	25.00	30.00
6.00	11.57	12.22	13.73	3.80	3.90	3.80	3.00	3.10	1.90
9.00	11.34	11.21	11.80	3.81	3.80	3.40	2.80	2.90	1.20
12.00	12.39	13.70	11.67	3.73	3.60	3.70	3.20	2.90	1.60
15.00	12.83	12.79	10.05	4.09	3.70	3.60	3.10	3.30	1.80
18.00	12.25	13.41	11.34	4.06	4.20	4.20	3.30	4.10	3.00
21.00	11.00	13.83	8.90	5.20	3.80	3.80	3.60	2.90	2.11
24.00	11.27	12.70	12.78	6.07	4.00	3.80	3.50	3.70	1.80
27.00	11.21	10.84	10.16	5.59	3.80	3.60	3.50	3.10	2.40
30.00	11.68	12.72	11.71	4.53	3.77	3.40	2.90	2.80	1.90
33.00	11.77	11.03	11.07	5.05	3.90	3.60	2.70	2.80	2.50
36.00	11.41	11.58	9.38	6.21	4.30	3.60	3.20	3.30	2.70
39.00	12.26	11.33	9.58	5.55	4.50	3.90	3.40	3.60	2.30
42.00	12.74	12.09	12.75	4.70	3.80	3.67	3.30	3.40	2.80
45.00	12.09	12.11	10.96	4.80	3.90	3.50	3.60	3.20	2.50
48.00	12.47	12.76	12.48	4.70	3.80	3.60	2.90	2.70	2.40
53.00	11.26	12.67	12.98	4.80	4.00	3.50	3.90	3.10	2.20
AVE.	11.85	12.32	11.33	4.79	3.92	3.66	3.24	3.18	2.19
SIGMA	0.56	0.90	1.37	0.76	0.22	0.19	0.33	0.37	0.47

Vo at 30 inches = 9.1 ft/sec
* transverse position from far wall in inches

15

B. MODEL

The 1/140 scale model was constructed from wood by a model-making vendor in the Philippines, and painted a flat black. It was made to scale using DD-963 blueprints provided by the Supervisor of Shipbuilding, Conversion and Repair in Pascagoula, Mississippi. Table 3 provides model and actual dimensions of the DD-963.

TABLE 3. SHIP/MODEL DIMENSIONS

	Model	Ship
Overall Length	4' (1.2 m)	563' 3 3/16" (171.7 m)
Beam	4.7" (11.94 cm)	55' (16.8 m)
Flight deck height above water	2.75" (6.98 cm)	32.5' (9.9 m)

The model was mounted directly to a mechanism specifically designed to provide dynamic simulation of pitch, roll and/or heave, however, this study was restricted to static conditions due to the model weight. A lighter model is on order, and dynamic studies will be pursued at a later date. The mount did provide, though, a relatively simple method of moving the model through the combinations of yaw, pitch and roll.

Foam weatherstripping around the tunnel floor cutout provided a seal against an inflow of air while the tunnel was running.

C. HELIUM BUBBLE GENERATION

Helium bubbles were generated by two, nearly identical sets of equipment. One is a Sage Action, Inc. console and bubble filter, and a second set was similar to the Sage Action model and constructed by department technicians. Each system can be schematically depicted as in Figure 10.
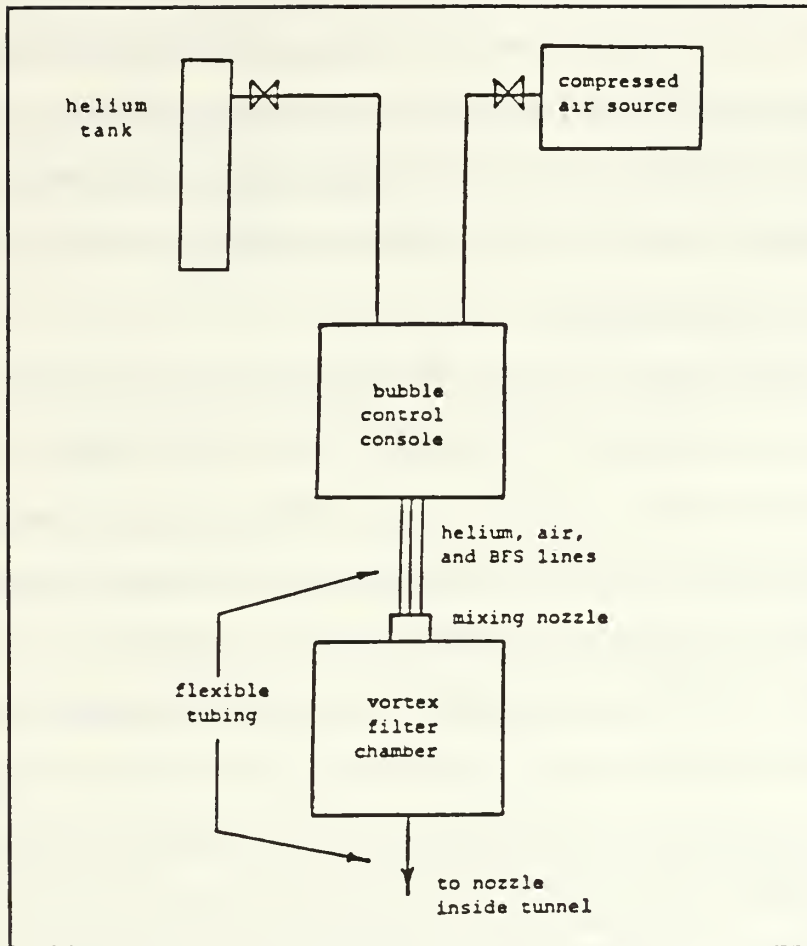
Figure 10. Schematic of Helium Bubble Generation System. [Ref. 13]

The systems utilize common compressed air and helium sources, and in each console a small, internal tank holds a bubble film solution procured from Sage Action. The bubble control console meters the components which are directed through flexible tubing to a bubble generating nozzle mounted on the bubble filter. The filter is a right circular cylinder, constructed of plexiglass, and in use contains the bubbles in a swirling motion. The filter functions by allowing the heavier bubbles to impact on the outer wall or fall to the floor of the filter, and the lighter ones to impact on the center tube. The bubbles that are neutrally buoyant remain

17

swirling and eventually are forced out the rigid center tube which extends from the top of the filter into the lower center. The collection tube is then fed to the variable position bubble jet outlets in the tunnel test section just forward of the model, and aft of the turbulence generating dowels. The outlets consist of rigid metal "guns" made of metal tubing and inject the bubbles in a direction parallel to the mean flow.

D. SMOKE GENERATION

Smoke was generated utilizing a theater fog machine manufactured by the Rosco Corp. that used their proprietary "fog juice." It produced a suitable dense cloud of vapor which reflected light quite well. The machine, as manufactured, is poorly equipped for flow-viz work. It is intended to generate large amounts of vapor, which immediately exits from the machine under almost zero pressure. Furthermore, the vapor, when generated is hot, and although it will pass through a short length of about 2" (50 mm) duct, the latter must be heat resistant and short enough to avoid condensation. A very satisfactory solution was to pass the vapor from the machine directly into a plastic drum about 40" (1 m) high and about 20" (0.5 m) diameter where it collected and became cooler. A small, variable speed in-line blower was attached to the drum and blew the cool, dry vapor along flexible plastic tubes about 0.125 - 0.2" (3-5 mm) diameter into the regions being studied.

E. LIGHTING

Light sources used were various combinations of Xenon arc lamps and quartz-halogen slide projectors. The arc lamps were procured from Sage Action, Inc., and Oriel Corp., and consisted of two 150 Watt, and two 300 Watt lamps with attached collimation optics. They supplied light with an optimum color temperature range of

5000 - 6000 Kelvin. Power supplies for the arc lamps allowed current variations, thus providing variable intensity lights.

To enable precise light placement on and around the model, standard 2X2 inch slides were used in the quartz-halogen slide projectors. Metallized tape was applied across blank slides and then cut out to fit the shape of the desired light beam.

The lights were placed two to five feet aft of the model and were considered to have an insignificant effect on the flow in the immediate vicinity of the model due to their small size; which ranged in height from 4 to 5 1/2 inches.

F . STILL PHOTOGRAPHY

Photographs were taken with a Hasselblad 2000 FCW medium format camera with Tessar 110 mm f2, and 150 mm f2.8 lenses. Accessories included a Bogen tripod, Polaroid film pack, and an A12, 120 size film pack.

G . VIDEO

Video equipment utilized included a Panasonic WV-1850, 800 line closed circuit camera with a 25mm f1.4 automatic iris lens, a Panasonic WV-5470, 850 line monitor, and a Mitshubishi HS-423UR, 440 line super-VHS video cassette recorder.

IV. EXPERIMENTAL PROCEDURE

With this initial flow visualization study conducted under time constraints, it was necessary to select only certain combinations of ship yaw, pitch and roll angles in the static mode. Considering a typical safe operating envelope such as Figure 5, and the fact that the given tunnel boundary layer simulated a 29 knot wind over the Spruance model in a developed sea, yaw angles of 330 - 030° in increments of 15° were chosen. In addition, ship roll extremes from 0 to 5° - port and starboard - and pitch extremes from 0 to 4° in pitchup were examined; pitchdown is left to a later study. The primary focus of the study was on the flight deck; however, the bow and mid-ship areas were investigated to a lesser degree.

Photographing the helium bubbles in a 3-d flowfield is a very tricky process, partly because the bubbles reflect only an estimated 5% of the incident light, and partly because the background, in this case the ship model, must be kept in subdued light. In essence, this translates into the need for intense white lights off the model, where the bubbles will be, and very little light on the model; collimation optics provide sharp edge definition and allow the light beam to be in close proximity to the model, without "washing" it out.

The greatest difficulty in visualization of turbulent flows is that the medium introduced to the fluid disperses rapidly shortly after its introduction. With aerosols, this usually means that the body becomes enveloped in a fog and, with helium bubbles, it means that the bubbles scatter and tend to avoid regions of greatest interest. Injection near the latter regions is often difficult to achieve, without disturbing the flow. Furthermore, working with 3-d flowfields is much more

demanding in terms of positioning the cameras and light sources than with 2-d ones. Great patience and skill is required to obtain good results.

As the observations progressed through many combinations of pitch and roll in the static mode, it became apparent that there was no significant differences detectable on the helium bubble photographs or video. Such differences may be detectable when the model is being oscillated to simulate the pitching and rolling - again left to a later study.
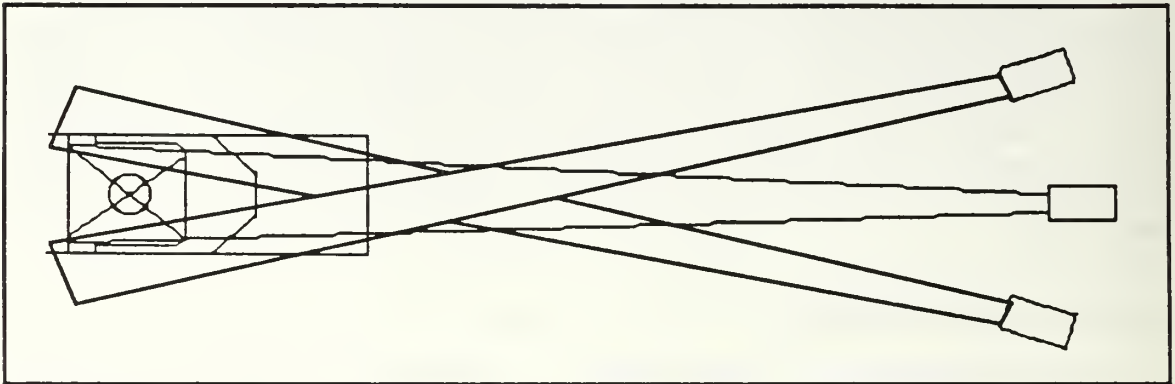
A. HELIUM BUBBLES

As described earlier, the helium bubbles were injected into the flow between the turbulence generating dowels and the model. Because of their dispersive nature, and in order to direct the bubbles to specific areas of interest, various lengths of 3/8" (9.5 mm) tubing were attached to the outlets and held parallel to the flow. This maximized the bubble concentrations where desired.

Lighting adjustments were consistently the most time consuming procedure. Optimally, light should illuminate the entire airspace of interest in the vicinity of the model, yet not fall on the model. This proved difficult because the flight deck/hangar area was not situated to allow simple lighting from astern without some reflection problems from the hangar. Lighting from the sides was ruled out due to problems encountered by Daley [Ref. 14 p.40] which resulted from crossing light paths and was corrected by using only parallel or nearly parallel light sources. Additionally, lighting from the side would directly interfere with photography from that same orientation.

The solution lay in using two strong light sources oriented as in Figure 11 and a light with less output oriented from directly astern, "flooding" the hangar. This illumination of the model surface proved not to be a detriment as long as the

photograph was taken from an aspect that was even with, or very slightly forward of, an imaginary plane that contained the hangar face, thereby allowing no direct reflections from the aft hangar face to reach the film.

Figure 11. Typical Lighting Arrangement for Helium Bubble Flow Visualization of Flight Deck.

Photography consisted of using the Hasselblad initially to take monochrome Polaroid (3000 ASA) pictures to determine the optimum exposure and following with Kodak TMAX, which is nominally ASA 400 monochrome and "pushed" to ASA 1600 in developing. Photographs were taken from two aspects:

- low, close to "profile" perspective, and
- a high angle – about 30° from the vertical

Most exposures were in the range f5.6 to f16 and 1/2 to two seconds. In addition, time exposures of 10 - 20 seconds were taken with a relatively weak light directly astern. The latter pictures were particularly effective in delineating vortical flow just aft of the hangar.

Video was taken from the same two perspectives plus directly overhead, and later edited. Lighting used for the video was modified slightly to compensate for the automatic iris feature on the camera lens. Two incandescent lamps positioned on top

of the tunnel, powered through a rheostat, provided variable intensity ambient light through the overhead window into the test section. Without this additional ambient light, the bubbles were "overexposed" as a result of the iris being at or near the full open position. Raising the ambient light level closed the iris slightly, properly exposing the bubbles.

B. SMOKE

Smoke was introduced "on" the model at three locations via small tubes routed alongside of the model from below the tunnel floor. One was on the top of the hangar, and the other two were on each side, all directing the smoke aft; Figure 12 depicts their location. The variable speed fan was maintained at a low enough level to prevent flow disturbance, yet provided sufficient quantities of smoke.
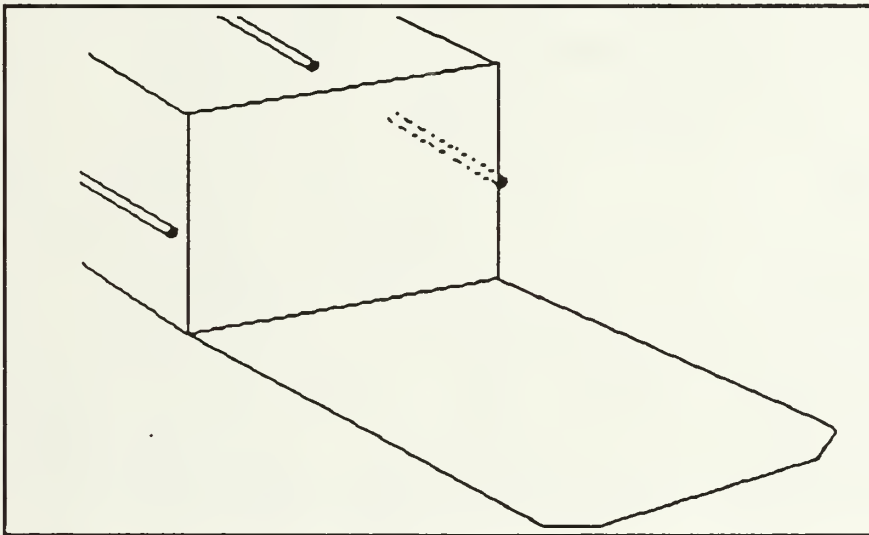

Figure 12. Hangar Smoke Tube Locations

Attempts at still photography of the flow visualized by smoke proved fruitless. All the smoke areas blended into each other with no discernible flow direction depicted.

Video, however, allowed excellent smoke flow-viz. Lighting consisted of one arc lamp at a fairly bright setting positioned directly astern, illuminating the entire flight deck area. In addition to video of the overall flow pattern with smoke emanating from all three tubes, localized analysis was conducted by clamping two tubes at a time. Video segments were taken from the same aspects as those taken in helium bubble video.

V.   RESULTS

The most notable feature of flows around 3-d bodies in a sheared turbulent flow is the formation of trailing vortices from almost every salient edge of the body. In general, the magnitude of the wake increases with the angle of yaw and is quite massive at 30° and greater. At small yaw angles, a small vortex trails downwind along the lee of the ship and grows in strength as the yaw angle increases; such vortical flow is shown in Figure 13, one of only a few photographs taken of the ship's mid-section.
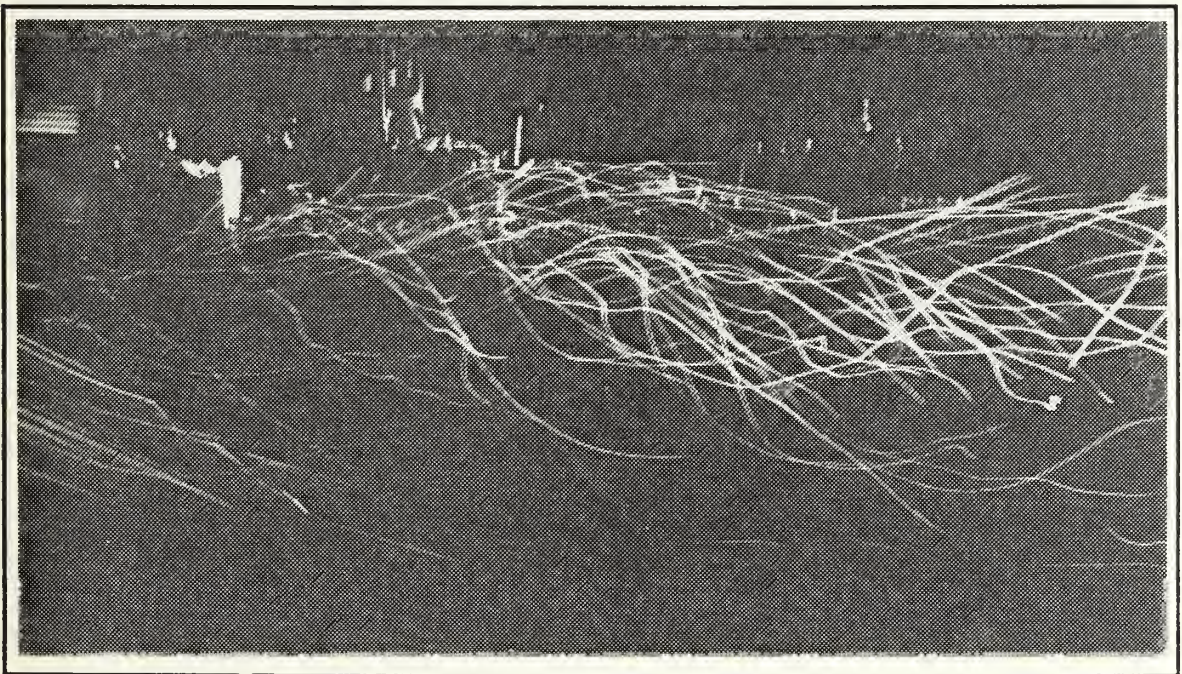
Figure 13. Vortex in the Lee of the Ship - 330° yaw, 4° pitch up, 5° starboard   roll.

During the course of this study the author operated the flow visualization tunnel over 100 hours, resulting in five hours of video, and over 300 "TMAX" photographs; with the bulk of the more significant results derived from the flight

deck smoke video. The entire set of photographs, (plus the Polaroid prints) and the video tapes remain at the Naval Postgraduate School in the custody of Professor J. V. Healey. The following sections will present a representative sampling of the photographic results, plus interpretive drawings of the video.

As discussed earlier, it was found that no qualitative differences in the flow could be discerned from varying pitch and roll while at the same ship yaw angle. Additional studies with a lighter model in dynamic pitch and roll will have to be conducted. Thus, in the following discussions, there is no attempt at pitch or roll analysis, but for completeness, the figure captions indicate at what ship attitude the photograph was taken at. Figures that refer to the photograph aspect as being "vertical" are actually photographs taken approximately 30° from vertical.

A. 030° YAW

This ship yaw angle corresponds to winds that are 330° relative across the flight deck which are typically those preferred by pilots because of the starboard side approach. Note that these winds are just within the day, starboard approach wind envelopes (Figure 5).

Figure 14 is a profile shot of the flight deck and indicates the general flow. Note the turbulence just aft of the hangar, and the vortices trailing off equipment/antennas on top of the hangar. As would be expected, the flow tends to "smooth" out as it progresses aft. Most results generally indicate that the transition region starts in line with the aft edge of the flight deck, and continues for a relatively short, variable distance aft.

Figures 15 and 16 show the flight deck from the vertical, with associated vortices over the flight deck and trailing off the superstructure above the hangar.
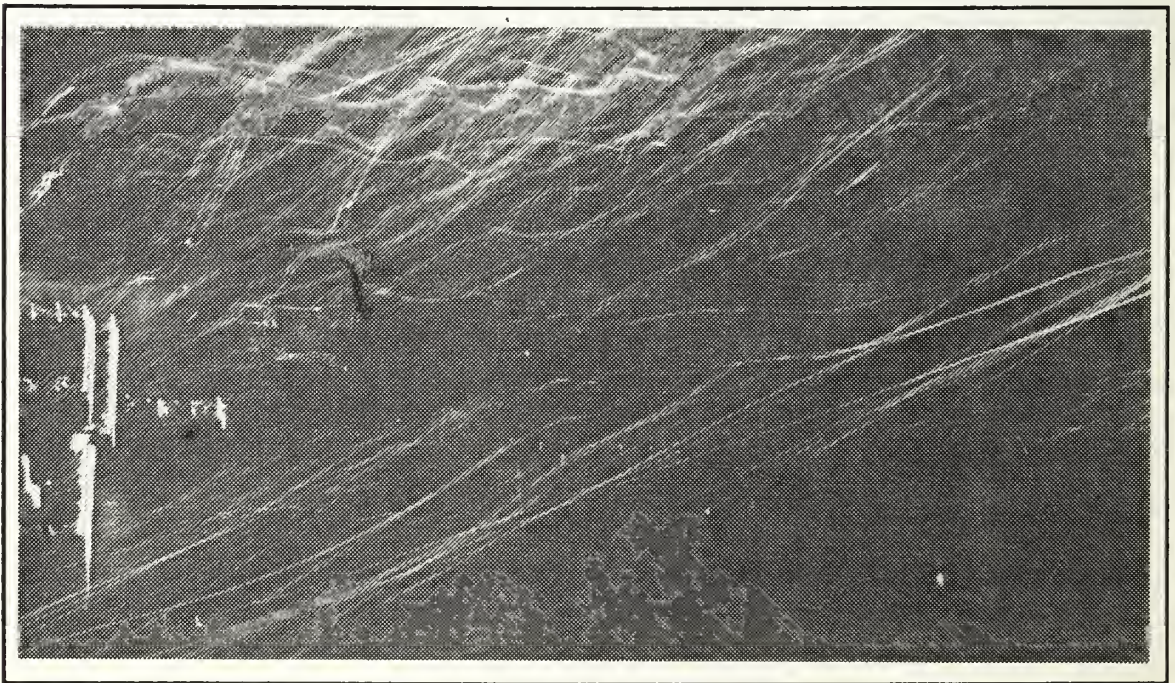
Note the relatively smooth flow in the "free stream" on the port side of the ship extending across the ship aft of the hangar.
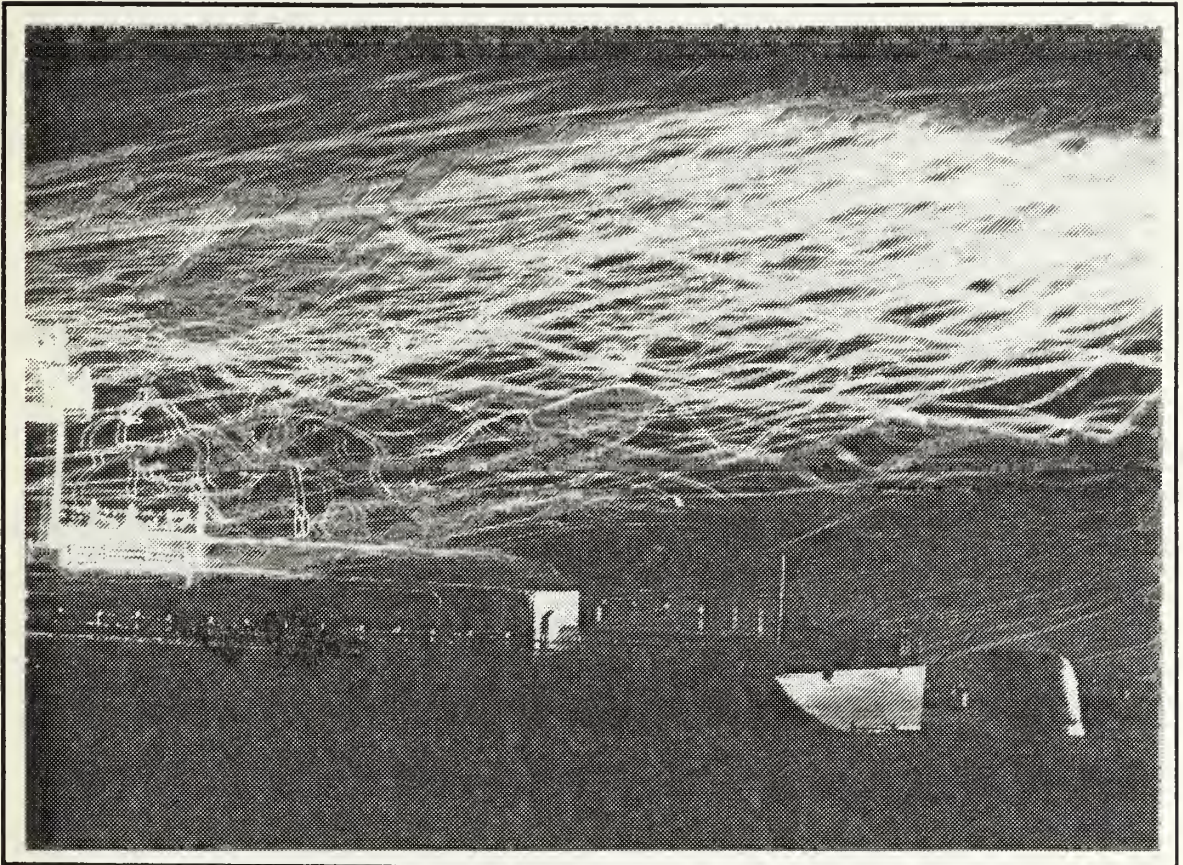
Figure 14. Wake of the hangar - 030° yaw, 4° pitch up, 5° starboard Roll.
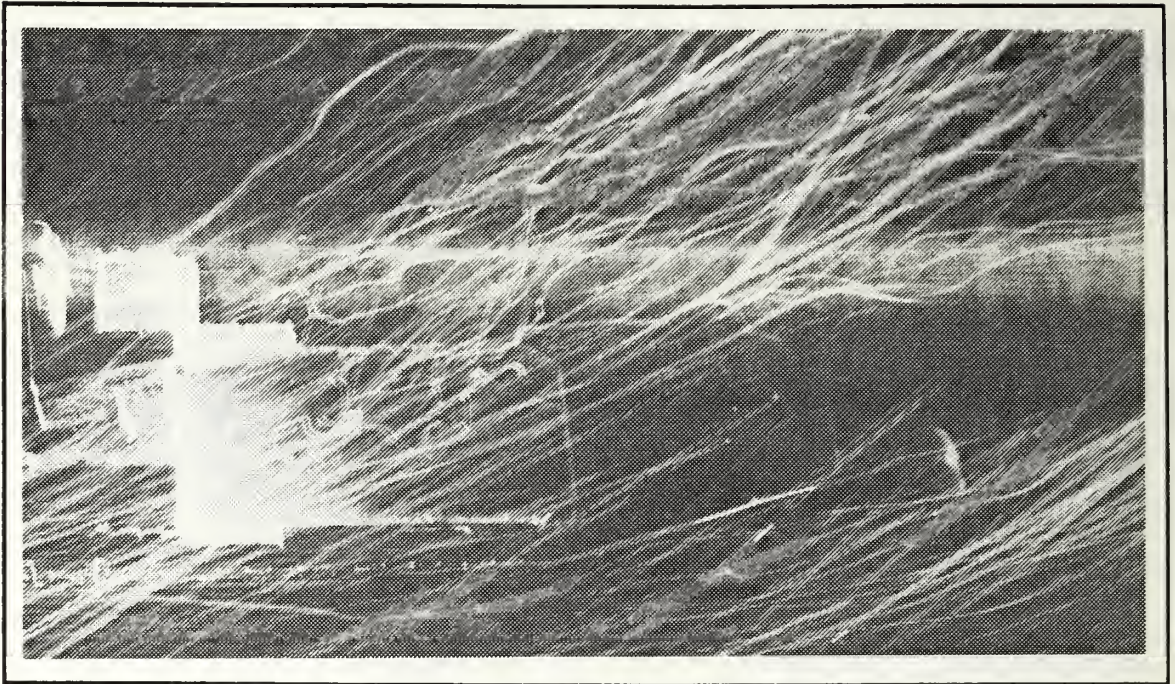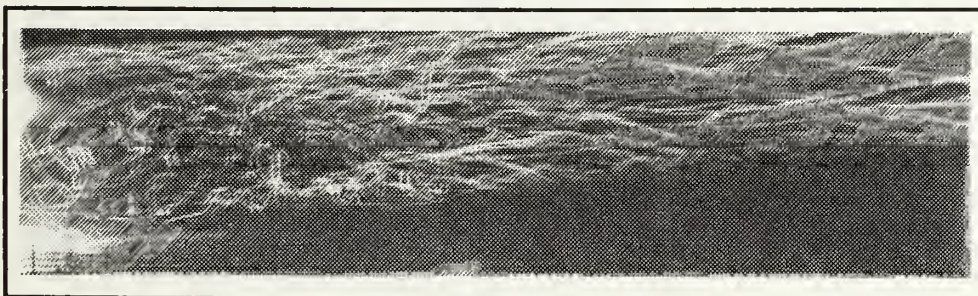
Figure 15. Wake of the hangar - 030° yaw,4° pitch up, 0° roll.

Figure 16. Wake of the Hangar - 030° yaw, 0° pitch, 0° roll.

The "turbulence" over the flight deck referred to in Figure 14 can be better described as part of a more general flow pattern consisting of a bound vortex circulating just aft of the hangar in a clockwise direction, as viewed in profile from the port side. Figures 17 and 18 are long time exposures, with the hangar at the left edge of the picture, which shows upper layers of the flow proceeding aft and the vortex formed by the flow moving downwards, back towards the hangar and upwards again. Note again how the flow starts to smooth out as it moves aft of the flight deck.
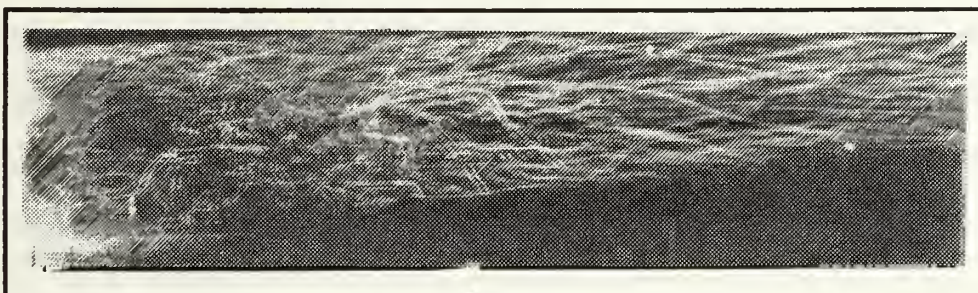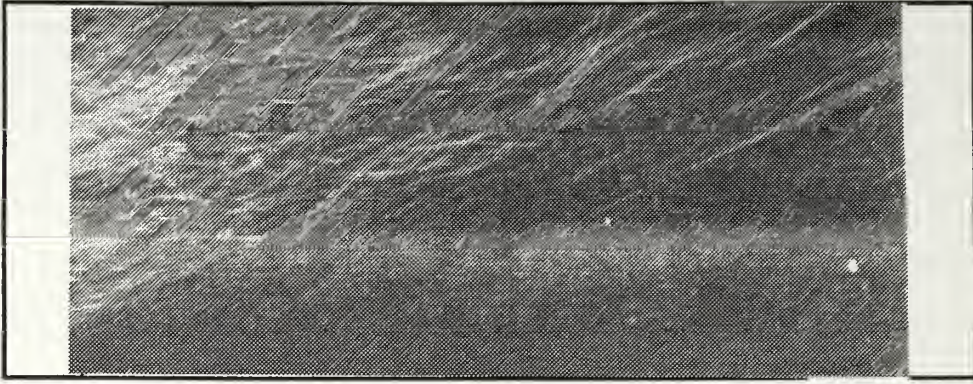

Figure 17. Typical Vortex Aft of Hangar - View from Port side - 030° yaw, 4° pitch up, 0° roll.


Figure 18. Typical Vortex Aft of Hangar - View from Port side - 030° yaw, 4° pitch up, 0° roll

Figure 19 is a time exposure of the flight deck taken from the vertical, with the free stream flow clearly "covering" about one third of the flight deck.

Figure 19. Typical Vortex Aft of Hangar - View from Vertical - 030° yaw, 0° pitch, 0° roll.

Figure 20 shows the general flow pattern, as ascertained by smoke introduction along the sides and top of the hangar. Such patterns are moderately easy to decipher from the video, but photograph poorly. Generally, they indicate that the airflow near the center line of the ship flows over the hangar and splits: the higher
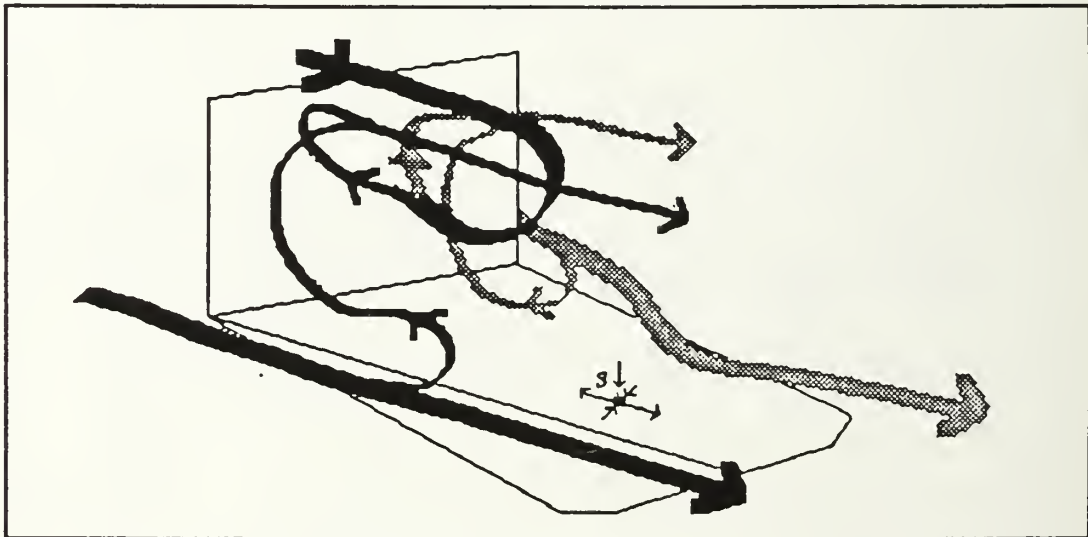

Figure 20. Flow pattern over flight deck at 030° yaw.

level of the flow continues aft and the lower level proceeds downwards towards the deck and turns back towards the hangar; this flow further splits, heading towards port and starboard, curls upward almost to the hangar "roof" level and

finally flows downwind in two streams along the direction of the free steam flow. Note again the area of the flight deck with smooth flow above. The "s" in Figure 20, and later figures, indicates the approximate location of the stagnation point.
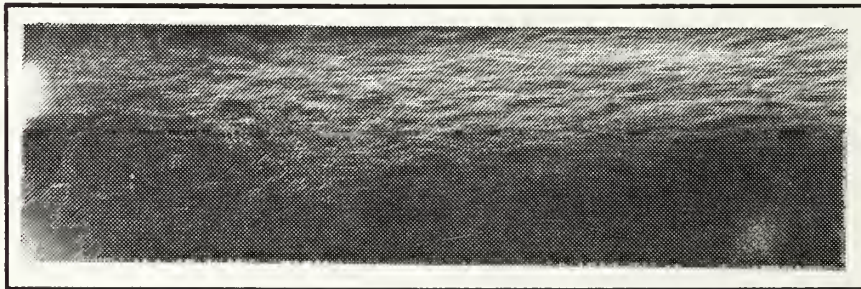
B. 015° YAW

When the ship turns more towards "winds on the bow", the flow becomes less turbulent, and the center of the bound vortex over the flight deck moves slightly aft. In addition, the apparent radius of curvature of the bound vortex becomes somewhat larger. Figures 21 - 24 illustrate these points when compared with Figures 14 - 19. Note in Figure 22 the bubble streak entering the flight deck flow pattern from the starboard side of the hangar and how it curves back in towards the hangar, up and then back aft. Note also in Figure 24 the shift in the free stream type flow that occurs over the flight deck, as compared with Figure 19.
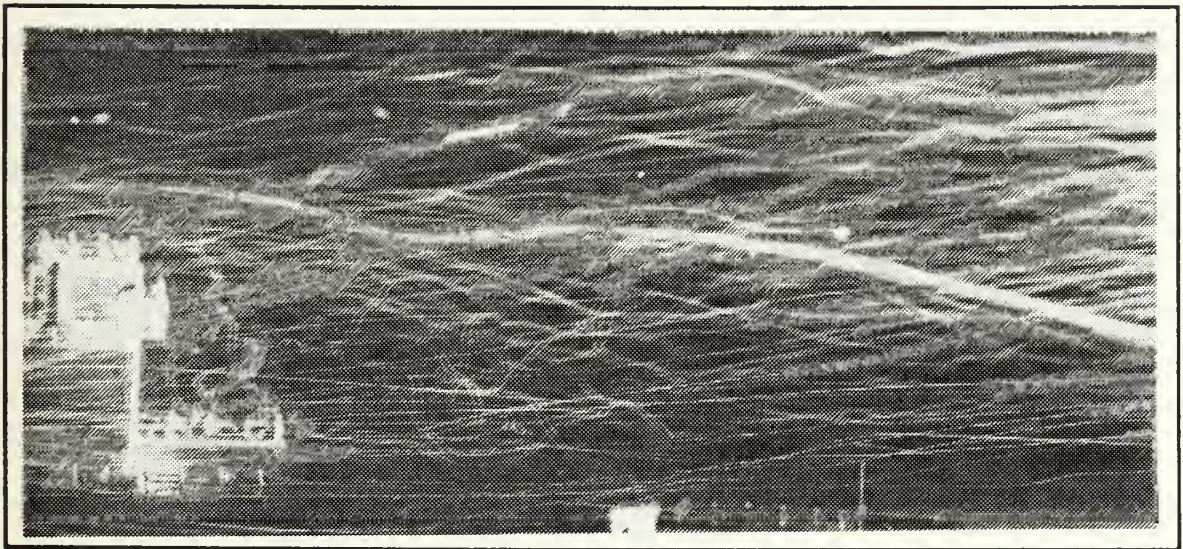
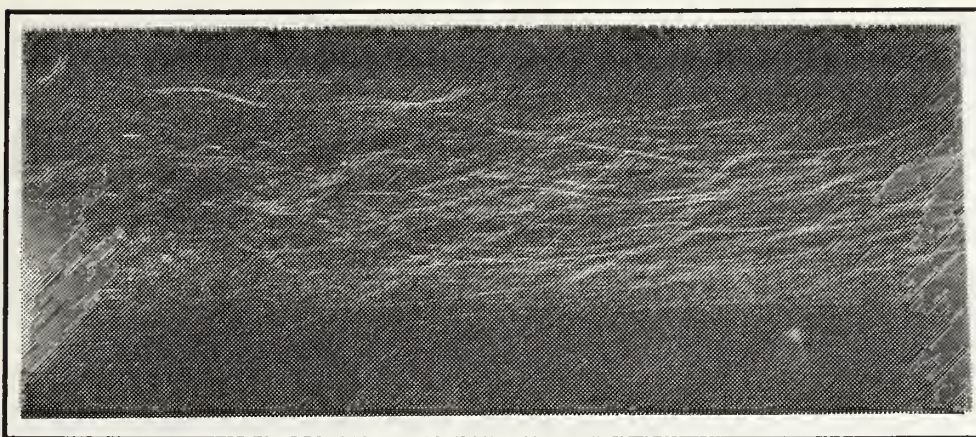**Figure 21. Wake of the hangar - 015° yaw, 4°pitch up, 0° roll.**
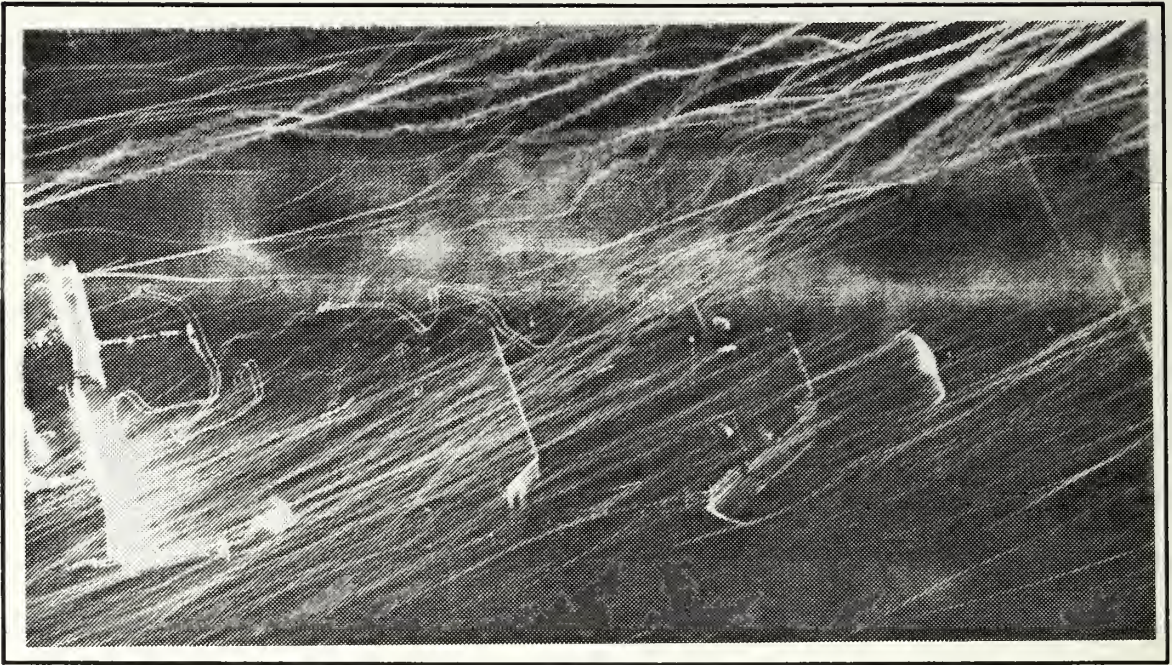
Figure 22. Wake of the Hangar - 015° yaw, 0°pitch , 0° roll.

Figure 23. Typical Vortex Aft of Hangar - Profile View from Port Side - 015° yaw, 4° pitch up, 5° port roll.
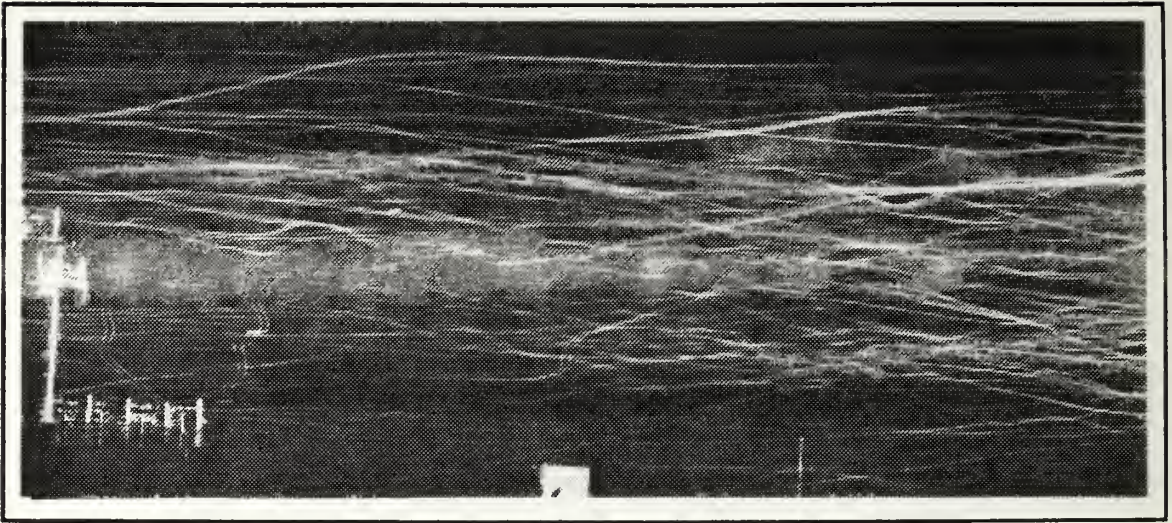
**Figure 24. Typical Vortex Aft of Hangar - View from Vertical - 015°
yaw, 4° pitch up, 5° starboard roll.**

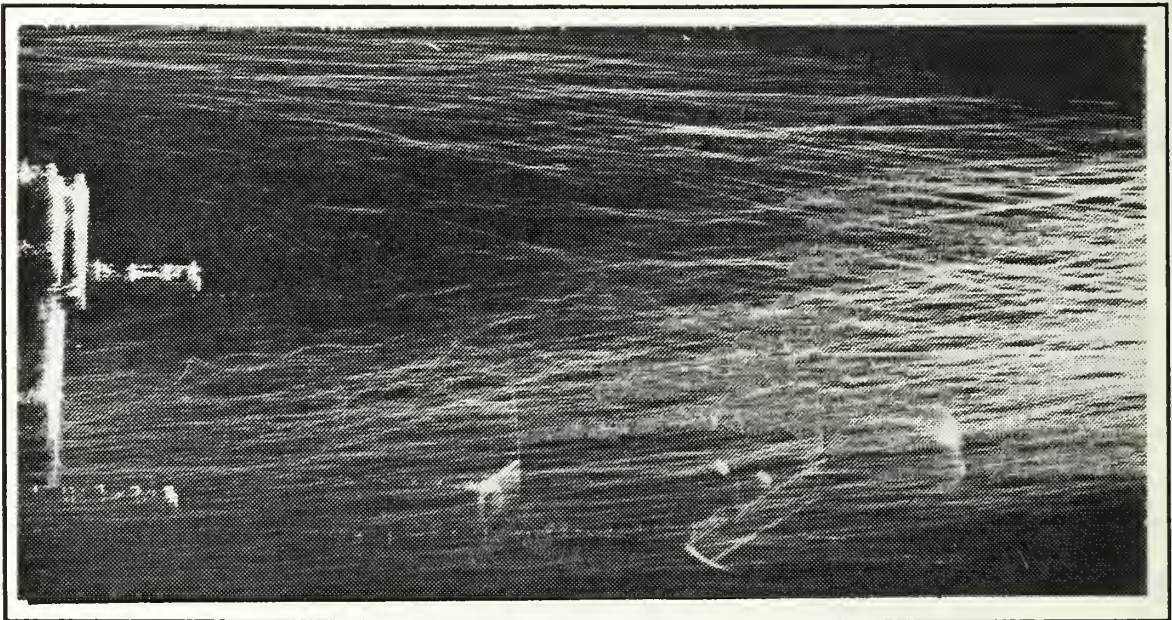## C. 000° YAW

With the air flow at 000° relative, the vortical movement is at its lowest overall intensity, with the center of the bound vortex over the flight deck at its furthest point aft. Figures 25 - 30 show the predominant, and relatively straight streaklines making up the smoother flow. Note that these results compare quite favorably with the fact that the maximum velocity winds allowed for landing are at, and in, the vicinity of 000° relative; as indicated in Figures 5 - 7.
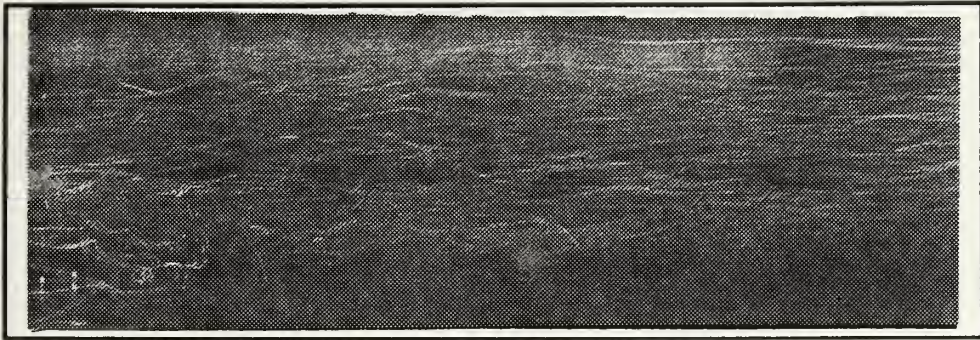
Figures 29 and 30 are included for general completeness, but illustrate no significant or unexpected flow patterns. Further work, however, is needed in the areas of the two VERTREP decks as stated earlier.

Figure 25. Wake of the Hangar - 000° yaw, 4° pitch up, 5° starboard roll.
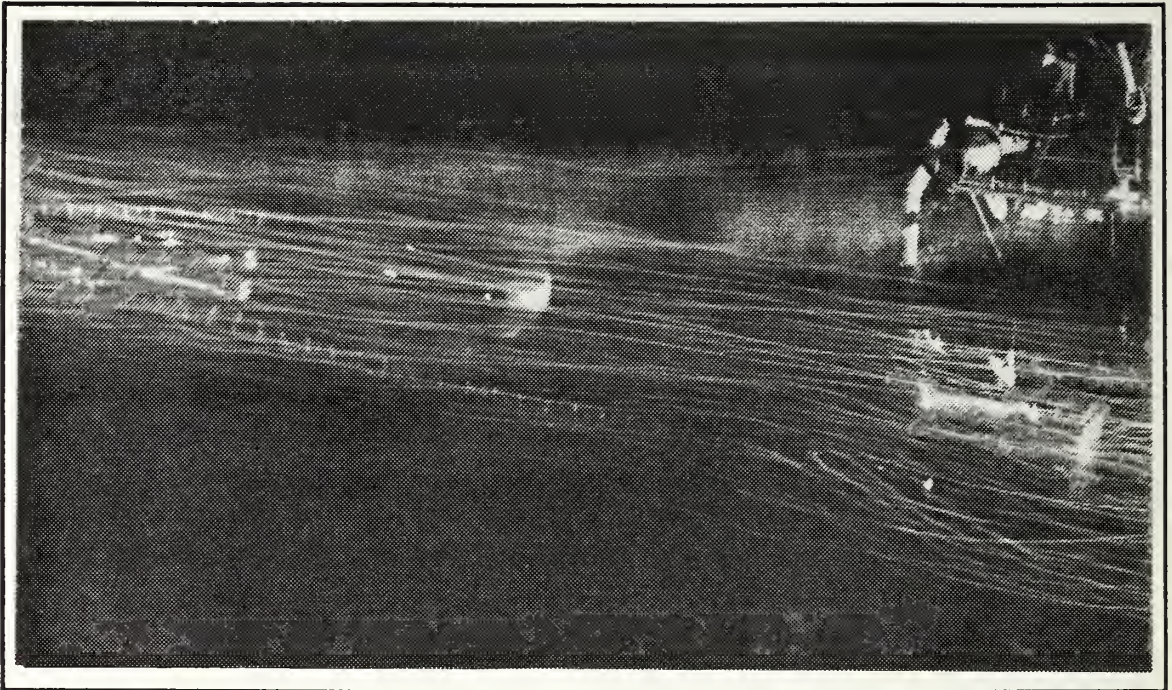

Figure 26. Wake of the Hangar - 000° yaw, 4° pitch up, 5° starboard roll.

Figure 27. Typical Vortex Aft of Hangar - Profile View from Port
Side - 000° yaw, 4°pitch up, 5° port roll.

Figure 28. Typical Vortex Aft of Hangar - View from
Vertical - 000° yaw,4°pitch up, 5° port roll.

Figure 29. Wake of Bow Area and Bridge Superstructure - View from Port Side - 000° yaw, 0° pitch, 0° roll.
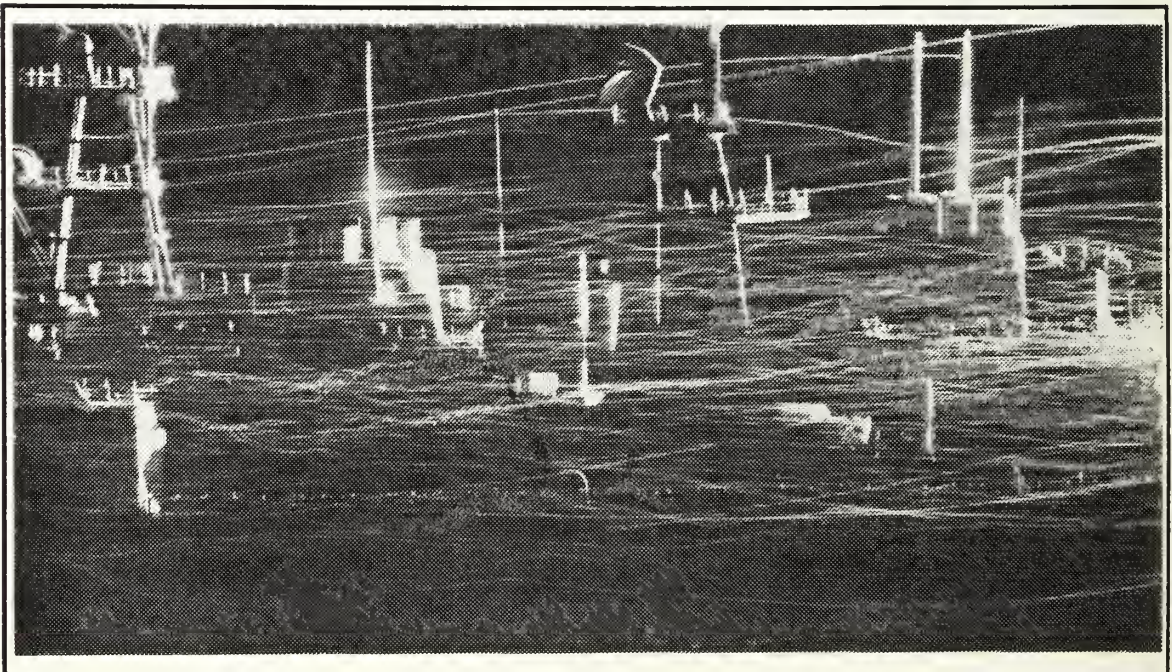
Figure 30. Wake of Midships Superstructure - View from Port Side - 000° yaw, 0° pitch, 0°roll.

The general flow pattern over the flight deck is illustrated by Figure 31, and is similar to the flow at 030° yaw with the following exceptions:

- The center of the bound vortex is positioned further aft over the flight deck at 000° yaw.
- At 030° yaw, the airflow coming off the hangar top shifts to starboard.
- The flow at 000° yaw is relatively symmetrical about the centerline while flow at 030° yaw is predictably canted to starboard, and not symmetrical about the 330° relative wind line.

Figures 32 and 33 are 2-d representations of the flow around the hangar from the top and from both sides. Note in Figure 33 the flow at 000° is not entirely symmetrical.
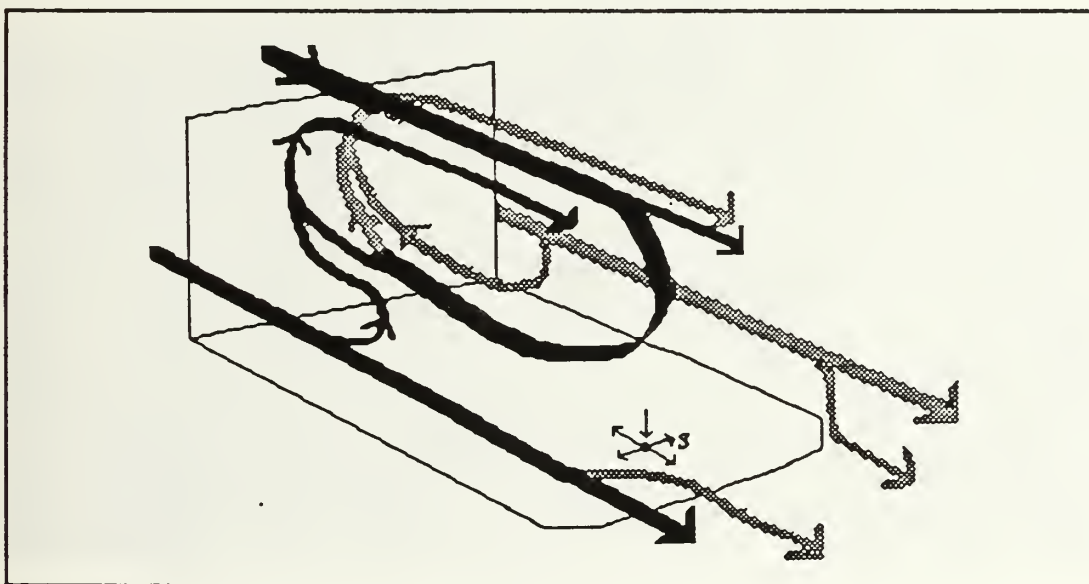

Figure 31. Flow Pattern over Flight Deck at 000° yaw.
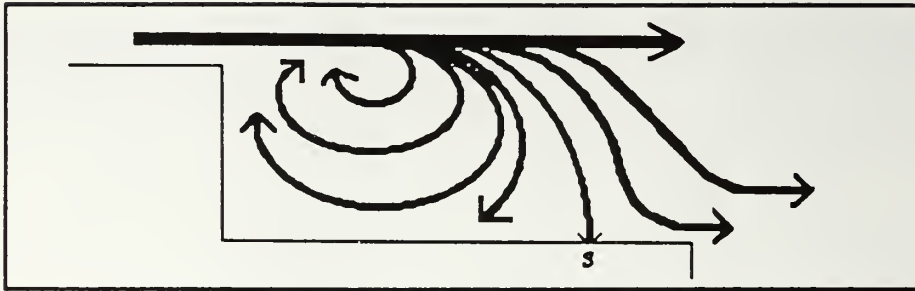
Figure 32. 2-d Flow Pattern over Flight Deck from Top of Hangar along Center Line of Ship at 000° yaw.
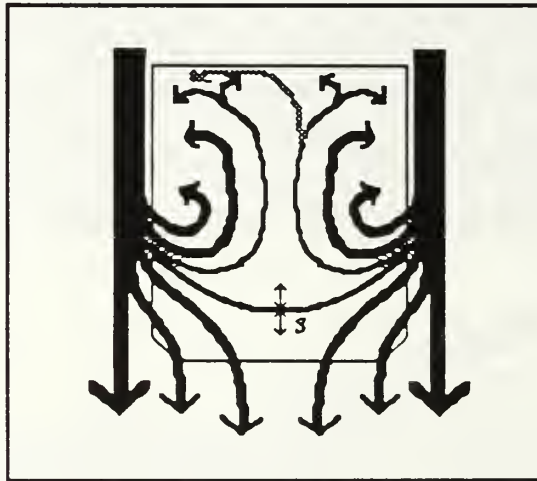
Figure 33. 2-d Flow Pattern near Flight Deck Surface from Sides of Hangar at 000° yaw.

D. 345° YAW

Using strictly helium bubble flow visualization, results for 345° yaw are essentially identical with those for 015° yaw, considering orientation (Figures 34 and 35). However, upon analysis of smoke video results it was realized that there are some differences which become even more apparent when the ship is at 330° yaw and will be discussed in the following section.
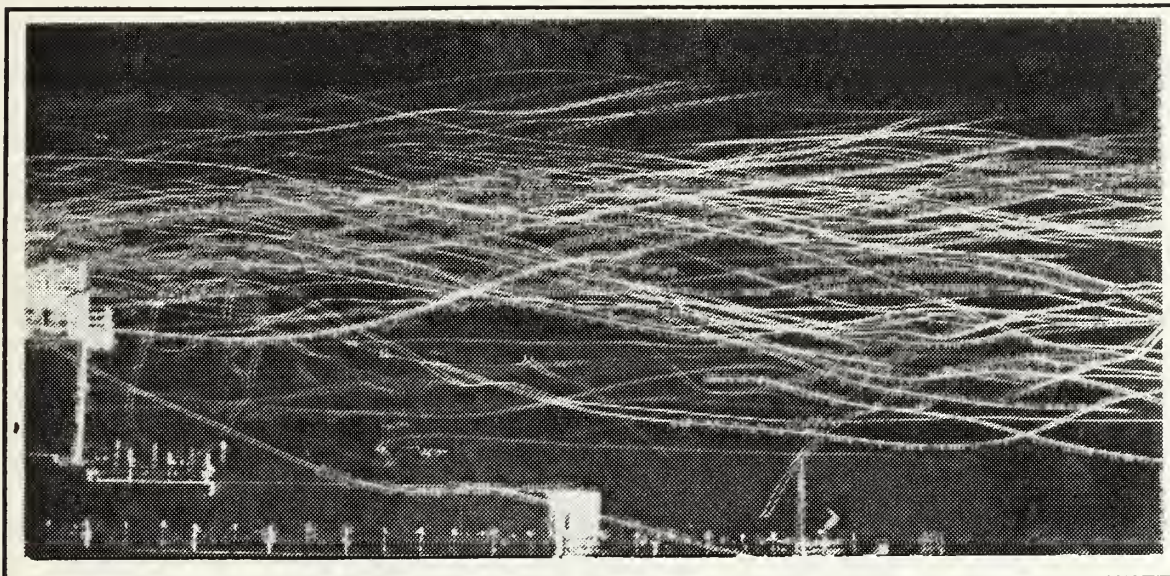
Figure 34. Wake of the Hangar - 345° yaw, 4° pitch up, 5° starboard roll.
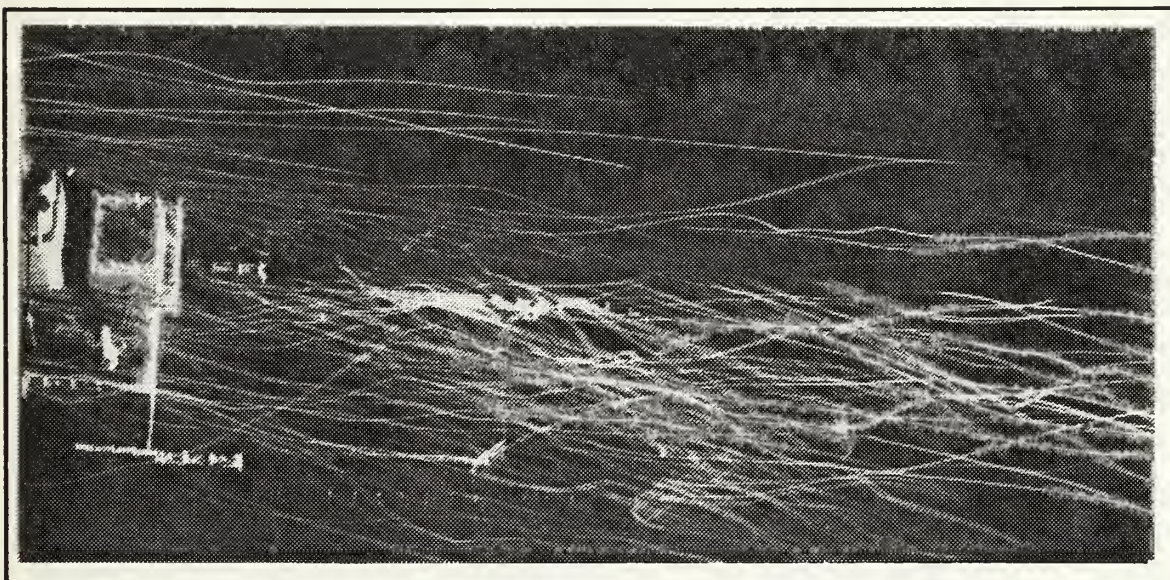
Figure 35. Wake of the Hangar - 345° yaw, 4° pitch up, 5° port roll.

E. 330° YAW

With the relative winds at 030° the airwake over the flight deck departs slightly from any symmetry expectations in relation to relative winds at 330°

(030° ship yaw). Due probably to the additional superstructure above the hangar on the starboard side (smoke "stack" and radar platform) the flow coming off the top of the hangar moves mostly upwards, slightly to starboard, and then proceeds aft. (Note that in 030° ship yaw, the flow also shifts slightly to starboard). A small amount of the flow acts as in the starboard and 000° yaws and curves downwards back towards the hangar; the radius of that curvature is much smaller than the other cases. Figure 36 shows the general flow pattern for this 330° yaw. Note again that about one third of the flight deck is exposed to relatively uniform free-stream flow. Also, additional analysis of overhead video segments with smoke revealed slightly more turbulence over the center portion of the flight deck than for 030° yaw. Figures 37 and 38 are flight deck helium bubble photographs with no direct analytical features other than the turbulence over the flight deck.
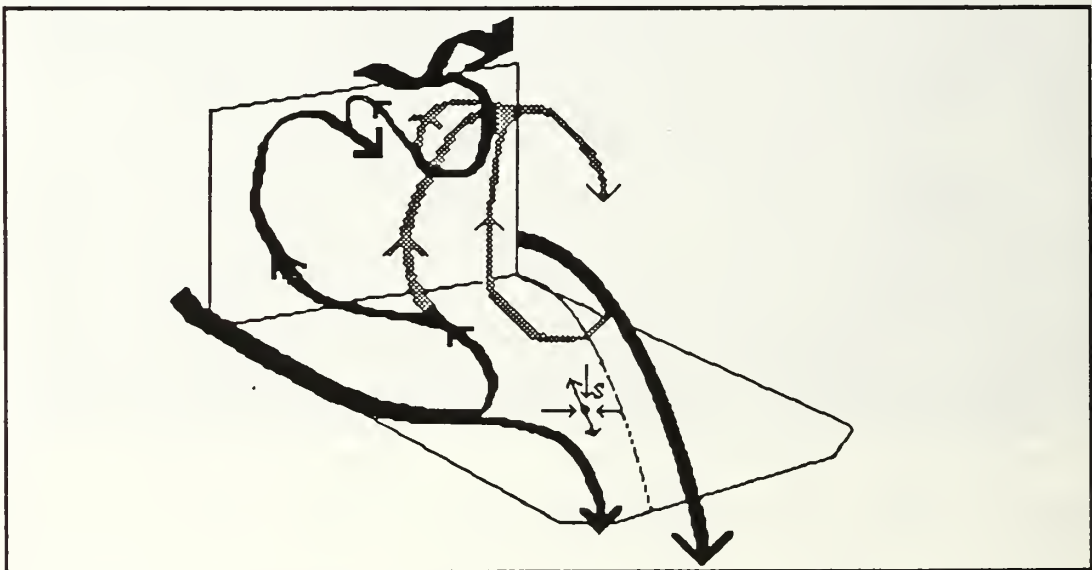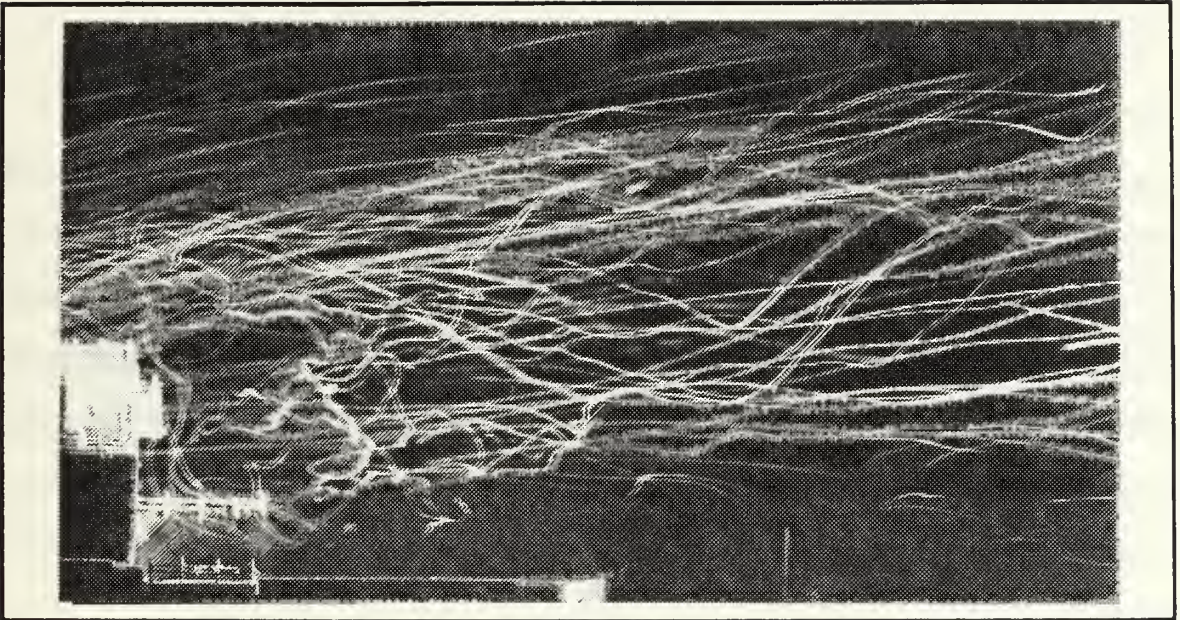

Figure 36. Flow Pattern over Flight Deck at 330° yaw.

Figure 37. Wake of the hangar - 330° yaw, 4° pitch up, 5° port roll.

Figure 38. Wake of the hangar - 330° yaw, 4° pitch up, 0° roll.

41

VI. CONCLUSIONS AND RECOMMENDATIONS

Utilizing helium bubble and smoke flow visualization techniques in a wind tunnel simulating the atmospheric boundary layer over an open ocean, the airflow over the flight deck was qualitatively defined and documented. While helium bubble visualization provided some initial definition of the overall flow, smoke flow visualization, utilizing video recording for later analysis, is by far the most productive technique. With insertion of smoke at strategic places in the flow, and close-in video analysis, one is able to obtain an extremely good picture of the flow patterns.

The air flow over the flight deck of the DD-963 can be described as being dependent on ship yaw, vortical in nature and extremely turbulent. Exact flow dependency on ship pitch and roll was unable to be determined in this static study, but at best it can be concluded that the effect is minimal.

The flow visualization techniques used, while quite effective, are just the first step in the eventual quantification of the mean flow leading to the determination of safe operating envelopes and other end products. To assist in these endeavors, the following recommendation are made:

- Conduct dynamic flow visualization studies using helium bubble, smoke, and minitufts, with concentration on the use of video and smoke techniques.
- Conduct further flow analysis on the approach paths to the flight deck, and VERTREP areas.
- Enlarge overhead viewing windows in the tunnel as much as possible, and construct a vibrationless camera mounting mechanism to obtain quality vertical photographic and video results.
- Calibrate the tunnel to ascertain the profiles and turbulence intensities at different free stream speeds.

42

- Utilize these flow visualization techniques, and follow on work in the conceptual and preliminary ship design phases in order to minimize the flight deck and approach path turbulence.

- Incorporate 3-d, video digital flow analysis, and hot-wire anemometry techniques in these types of studies.

- Conduct feasibility studies into the possibility of using the eventual quantified flow results in shipboard automatic approach/landing systems.

- Develop a series of short video tapes for distribution to helicopter squadrons and ships explaining and illustrating what is happening to the air flow around their particular ship(s). At the very least, training tapes of this nature should be incorporated into every helicopter fleet replacement squadron's syllabus.

LIST OF REFERENCES

1.   Healey, J. Val., "The Prospects for Simulating the Helicopter/Ship Interface", *Naval Engineer's Journal,* Vol. 99, No. 2, pp 45-63, March 1987.

2.   Cermak, J., "Aerodynamics of Buildings", *Annual Review of Fluid Mechanics,* Vol.8, pp 75-106, 1976.

3.   Davenport, A. G., in *Engineering Meteorology*, E. J. Plate, Editor, Amsterdam, Netherlands, pp 527-569, Elsevier Scientific Publishing Company, 1982.

4.   Naval Ship Research and Development Center Report 2368, *Comparison of Full Scale and Model Data of the Wind Velocity Over the CVS 16 Flight Deck*, by H. E. White and D. R. Chaddock, April 1967.

5.   Naval Ship Research and Development Center Aero Lab Report 1131, *Effect of an Ambient Turbulence Component on Model Carrier Turbulence Data,* by S. Loezos, 1967

6.   Boeing Vertol Report D210-11140-1, *Investigation to Study the Aerodynamic Ship Wake Turbulence Generated by an FF-1052 Frigate*, by T. S. Garnett Jr., December 1976.

7.   Boeing Vertol Report D210-11545-1, *Investigation to Study the Aerodynamic Ship Wake Turbulence Generated by a DD-963 Destroyer*, by T. S. Garnett Jr., August 1979.

8.   Naval Air Engineering Center report NAEC-91-8030, *Smoke Tunnel Study of a 1/200 Scale DD-963 Ship Model,* by T. S Garnett, 19 June 1984.

9.   Hurst, D. W., and S. J. Newman, "Wind Tunnel Measurements of Ship Induced Turbulence and the Prediction of Helicopter Rotor Blade Response", *Eleventh European Rotorcraft Forum,* London, England, pp 99-1 - 99-15, September 1985.

10.   E.S.D.U. Data Items 74030, 74031, Engineering Sciences Data Unit International, Suite 200, Chain Bridge Road, McLean, Virginia, 22101.

11.   Plate, E. J., *Engineering Meteorology*, pp 573-636, Elsevier Scientific Publishing Company, 1982.

12.   Bolinger, W. K., *Visualization of the Flow Field Around a Generic Destroyer Model in a Simulated Turbulent Atmospheric Boundary Layer,* Master's Thesis, Naval Postgraduate School, Monterey, California, June 1987.

13.   Biskaduros, J. L., *Flow Visualization of the Airwake of an Oscillating Generic Ship Model,* Master's Thesis, Naval Postgraduate School, Monterey, California, December 1987.

14.   Daley, W. H. III, *Flow Visualization of the Airwake around a model of a TARAWA Class LHA in a Simulated Atmospheric Boundary Layer,* Master's Thesis, Naval Postgraduate School, Monterey, California, June 1988.

15   Friedman, N., *U. S. Destroyers: An Illustrated Design History*, p. 370, Naval Institute Press, 1982.

16.   Naval Air Engineering Center NAEC-ENG-7526 Rev AF, *Shipboard Aviation Facilities Resume,* Department of the Navy, Naval Air Engineering Center, Lakehurst, New Jersey, p.107, 1 April 1988.

17.   Naval Warfare Publication (NWP-42 Rev. G,) *Shipboard Helicopter Operating Procedures* , App B, Washington, D.C., Department of the Navy, December 1986.

INITIAL DISTRIBUTION LIST

No. Copies

1. Defense Technical Information Center   2
    Cameron Station
    Alexandria, Virginia 22304-6145

2. Library, Code 0142   2
    Naval Postgraduate School
    Monterey, California 93943-5002

3. Department Chairman, Code 67   1
    Department of Aeronautics and Astronautics
    Naval Postgraduate School
    Monterey, California 93943-5000

4. Commander   1
    Naval Air Systems Command
    Air Vehicle Division
    Attn: Mr. Jonah Ottensoser, Code Air 53011C
    Jefferson Plaza 2, Rm. 904
    Washington, D.C., 20361

5. Mr. Bernard Ferrier   1
    CANDAIR LTD.
    1800 Laurentieu Blvd.
    Saint Laurent
    Quebec, Canada   H4R1KZ

6. Naval Air Test Center   1
    Attn: Mr. Dean Carico, Code RW40A
    Patuxent River, Maryland   20670

7. Naval Air Test Center   1
    Attn: Mr. Jerry Higman, Code RW81
    Patuxent River, Maryland   20670

8. Dr. J. Val Healey, Code 67He   6
    Department of Aeronautics and Astronautics
    Naval Postgraduate School
    Monterey, California   93943-5000

9. Mr. R.A. Feik   1
    Aeronautical Division
    Aeronautical Research Laboratories
    506 Lorimer Street
    Fisherman's Bend
    Box 4331 P.O.
    Melbourne, Victoria 3001
    Australia

10. Ms. Susan Bales   1
    Office of the Chief of Naval Operations
    Navy Department
    Washington, D.C. 20360-5100

11. LCDR Michael K. Johns   2
    3814 Marquis Place
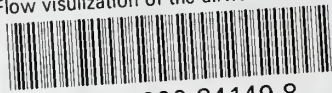   Woodbridge, Virginia 22192